[AMERICAN JOURNAL OF SCIENCE, VOL. 286, SEPTEMBER, 1986, P. 540-575]

FLUID BEHAVIOR AND PHASE RELATIONS IN THE SYSTEM Fe–Mg–Si–C–O–H: APPLICATION TO HIGH GRADE METAMORPHISM OF IRON-FORMATIONS

TAKASHI MIYANO* and CORNELIS KLEIN**

ABSTRACT. The phase relations of quartz, magnetite, siderite, grunerite, olivine, and orthopyroxene in the system Fe–Mg–Si–C–O–H are evaluated on the basis of available petrologic, experimental, and thermodynamic data. These phase relations can be used to estimate fluid compositions, fluid behavior, and mineral stabilities during high-grade metamorphism of Precambrian iron-formations.

The predominant gas species during high-grade metamorphism are CO_2 and H_2O, with other species present only in small amounts. Minor amounts of graphite in iron-formations produce only minor amounts of reduced species such as CH_4 and H_2. The phase relations can therefore be evaluated on T-X(CO_2) diagrams at Ps = P(CO_2) + P(H_2O). As a result of the compositional constraints on olivine and orthopyroxene in iron-formations, orthopyroxene ($0.6 < X_{Fe}^{opx} < 0.8$) cannot coexist with olivine at pressures above 2 to 5 kb, in the presence of magnetite. The topology of the phase relations can be divided into three types: (A) orthopyroxene-free and olivine-bearing assemblages (<2-5 kb, >400°C), (B) orthopyroxene- and olivine-bearing assemblages (<2-5 kb, >550°C), and (C) orthopyroxene-bearing and olivine-free assemblages (>2-5 kb, >550°C). These correlate well with mineral assemblages in various medium- and high-grade metamorphosed iron-formations.

The estimated fluid compositions for various metamorphosed iron-formations commonly show a wide range of X(CO_2), probably as the result of steep CO_2 and H_2O gradients. Our evaluation of several iron-formations suggests that fluid composition (X(CO_2)) is effectively controlled by the chemical composition (X_{Fe}) of the iron-bearing minerals rather than by temperature and pressure.

INTRODUCTION

Carbonates (calcite, siderite, ankerite) have been described from high-grade metamorphosed iron-formations (above 600°C) by many authors (for example, French, 1968; Haase, 1982a; Klein, 1983). Generally calcite and ankerite are the most abundant carbonates in the high-grade rocks, with siderite of only minor importance. The significance of carbonates during high-grade metamorphism of iron-formations has been discussed by Kranck (1961), French (1968), Butler (1969), Klein (1973, 1978), and Haase (1982a, b). Most of the authors conclude that H_2O and CO_2 have not behaved as perfectly mobile components during metamorphism. Burt (1972), Miyano (1976), and Floran and Papike (1978) have presented qualitative stability relations of iron-bearing minerals in the system Fe–Si–C–O–H in the presence of graphite and/or magnetite. Mel'nik and Shirostan

* Institute of Geoscience, The University of Tsukuba, Ibaraki 305, Japan
** Department of Geology, The University of New Mexico, Albuquerque, New Mexico 87131

(1973), Miyano (1978a, b, c), and Frost (1979a) quantitatively evaluated the phase relations of minnesotaite, grunerite, fayalite, and siderite in low- to high-grade metamorphosed iron-formations. Haase (1982b) made a detailed analysis of the phase relations in a six-component system applicable to iron-formations based on geometric-chemographic techniques and data from natural occurrences. In these theoretical studies, the stability of orthopyroxene, which is more common than olivine in high-grade metamorphosed iron-formations, was not evaluated quantitatively. Therefore, an assessment of the phase relations involving orthopyroxene is required for a realistic physicochemical analysis of high-grade metamorphism of iron-formations. It is the purpose of this paper to construct more complete phase relations in the system Fe–Mg–Si–C–O–H and to evaluate fluid composition and fluid behavior during high-grade metamorphism.

ACTIVITY-COMPOSITION RELATIONS

Well-established activity-composition relations for Fe-Mg olivine, orthopyroxene, grunerite, and siderite are essential to an evaluation of high temperature and pressure phase equilibria in the system Fe–Mg–Si–C–O–H.

The activity a_{Fe}^{ol} of olivine can be expressed as:

$$a_{Fe}^{ol} = (X_{Fe}^{ol} \cdot \gamma_{Fe}^{ol})^2 ,$$

where X_{Fe}^{ol} and γ_{Fe}^{ol} denote the mole fraction and activity coefficient of the Fe-endmember, respectively. The non-ideality of olivine solid solutions has been investigated by Nafziger and Muan (1967), Kitayama and Katsura (1968), Williams (1972), Kawasaki and Matsui (1977), O'Neill and Wood (1979), and Engi (1980). They showed a slight deviation from ideality above $X_{Fe}^{ol} > 0.7$ and at high temperatures (700°-1200°C). Fonarev (1981a), however, shows a greater deviation from ideality than any other workers and applied a symmetric solution model to his compositional data. Wood and Kleppa (1981) measured the enthalpies of solution of synthetic (Mg_2SiO_4–Fe_2SiO_4) olivine solution and concluded that the solid solution between the two endmembers exhibits small positive deviations from ideality. They gave the following equation for the evaluation of activity coefficients:

$$RT \ln\gamma_{Fe}^{ol} = \{W_{Fe} + 2X_{Fe}^{ol}(W_{Mg}-W_{Fe})\}(1-X_{Fe}^{ol})^2 \qquad (1)$$

where W_{Fe} and W_{Mg} are interaction parameters in an asymmetric solution model and 2000 and 1000 cal mol^{-1}, respectively. The estimated activity coefficient using this equation covers the temperature range from 700° to 1200°C.

Orthopyroxene solid solution has been investigated by Navrotsky (1971), Saxena (1973), Sack (1980), and Fonarev (1981a). They conclude that orthopyroxene behaves as a nearly ideal solution at the temperature range of 900° to 1200°C. At lower temperatures, Saxena (1973) showed significant positive deviation from ideality, and Navrotsky (1971) and Sack (1980) significant negative deviations. On the other hand, Fonarev's model

shows a positive deviation below 900°C and a slight negative deviation at 1000°C. Recently Chatillon-Colinet and others (1983) studied the thermochemistry of synthetic Fe-Mg orthopyroxene in terms of enthalpy of solution measurements in eutectic $(Li,Na)_2B_2O_4$ melts. They found that departures from ideality of the Gibbs energy of mixing in orthopyroxene are very small at temperatures of 700° to 1000°C. As a result, the activities of $MgSiO_3$ and $FeSiO_3$ may be replaced by their mole fractions at all temperatures in most petrologic calculations.

Because of limited experimental data for grunerite and siderite, activity-composition relations for these two solid solution phases are evaluated, as a first approximation, by two-site and one-site ideal mixing models, respectively. The two-site (M4 and M1,2,3 (set of sites M1,M2,M3)) mixing of a grunerite solution was modeled by Mueller (1962), Hafner and Ghose (1971), and Ghose and Weidner (1971). Hafner and Ghose (1971) and Ghose and Weidner (1971) showed that the Fe-Mg distribution in the M4 and M1,2,3 sites in the cummingtonite-grunerite series

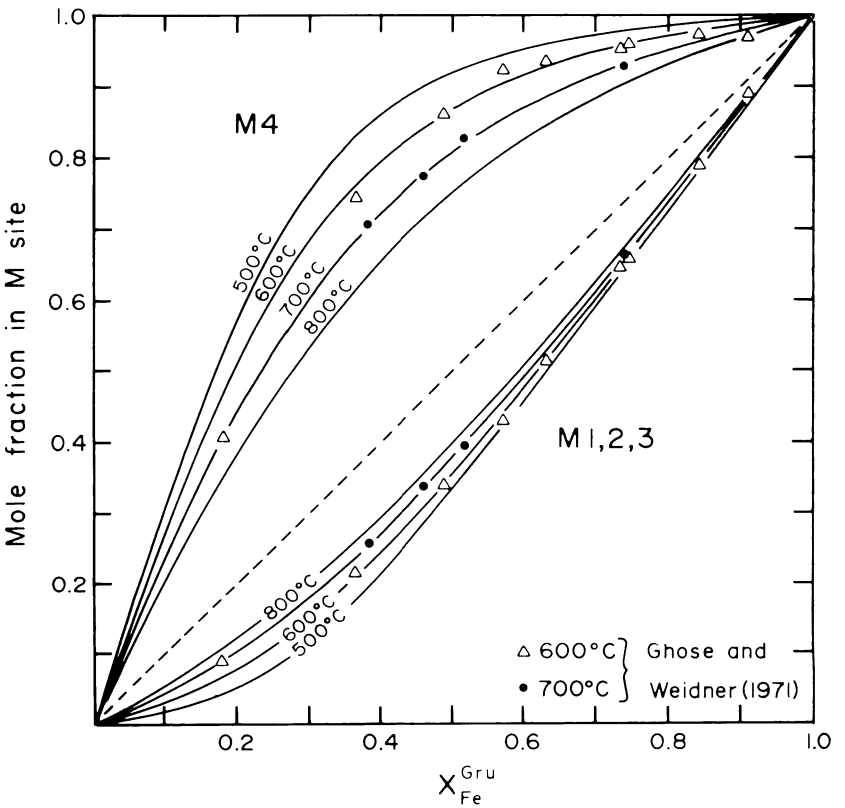

Fig. 1. Fe^{2+}–Mg^{2+} distribution isotherms in grunerite as a function of X_{Fe}^{gru}. The isotherms were calculated from experimental data of Ghose and Weidner (1971), on the basis of ideal mixing of M4 and M1,2,3 sites.

follows ideal-mixing behavior in these sites. Using the data of Ghose and Weidner (1971) and Ghose (1981), the Fe-Mg distribution in the M4 and M1,2,3 sites can be illustrated as a function of total mole fraction X_{Fe}^{gru} of grunerite (fig. 1). Extrapolations of these data to low- and high-temperature can be obtained by the following regression equation:

$$\ln K_D^{M4\text{-}M123} = -4578.59/T(K) + 2.76$$

where $K_D^{M4\text{-}M123}$ is the Fe-Mg distribution constant $(X_{Fe}^{M1,2,3} \cdot X_{Fe}^{M4})/(X_{Fe}^{M4} \cdot X_{Mg}^{M1,2,3})$ in M4 and M1,2,3 sites, and T(K) is temperature in degrees kelvin. The curves in figure 1 were obtained using this equation; X_{Fe}^{M4} and $X_{Fe}^{M1,2,3}$ at a given X_{Fe}^{gru} can be read from the figure. Thus, the activity of grunerite a_{Fe}^{gru} may be expressed as follows:

$$a_{Fe}^{gru} = (X_{Fe}^{M4})^2 (X_{Fe}^{M1,2,3})^5$$

Fonarev (1981b) estimated the thermodynamic properties of cummingtonite solid solutions on the basis of unreversed experimental data at 600° to 800°C from Fonarev, Korolkov, and Dokina (1976, 1979), Fonarev and Korolkov (1980), and mixing parameters of olivine and orthopyroxene of Fonarev (1981a), using an asymmetric solution model. He used compositions of coexisting minerals in the assemblages Cum–Opx–Qtz, Cum–Ol–Qtz, and Cum–Mt–Qtz. The results show negative deviations from ideality below 750°C and small positive deviations at higher temperatures. Compared with the two-site mixing model of this study, there is much greater deviation from ideality in Fonarev's model. Such deviation may well be due to the difficulty in attaining equilibrium in the experiments of Fonarev. His compositional data on coexisting synthetic olivine and orthopyroxene at 700° to 800°C (Fonarev, 1981a) are inconsistent with those from rocks and other experiments. The compositions fluctuate widely, a tendency similarly found in the data at 800°C of Bohlen and Boettcher (1981). As a result, the activity-composition relations of olivine and orthopyroxene appear to show greater deviation from ideality than suggested by the recent studies of Wood and Kleppa (1981) and Chatillon-Colinet and others (1983). This may amplify the deviation from ideality in Fonarev's model of cummingtonite. Based on Mueller's (1962) suggestion that geometrically similar sites in different silicates have similar energetic properties, grunerite (and/or cummingtonite) may have solution behavior similar to orthopyroxene (Ganguly, 1982). This means that cummingtonite-grunerite solution may well be close to ideal.

Siderite in high-grade metamorphosed iron-formations contains variable amounts of MgO, MnO, and CaO (for example, Butler, 1969; Klein, 1978). We assume, as did Mueller (1973), that siderite is an ideal solid solution between $FeCO_3$ and $MgCO_3$.

ACTIVITY-TEMPERATURE RELATIONS

Activity-temperature relations of mineral solid solutions in the system Fe–Mg–Si–C–O–H can be computed on the basis of the activity-composition relations discussed above. Figure 2 depicts activity-temperature rela-

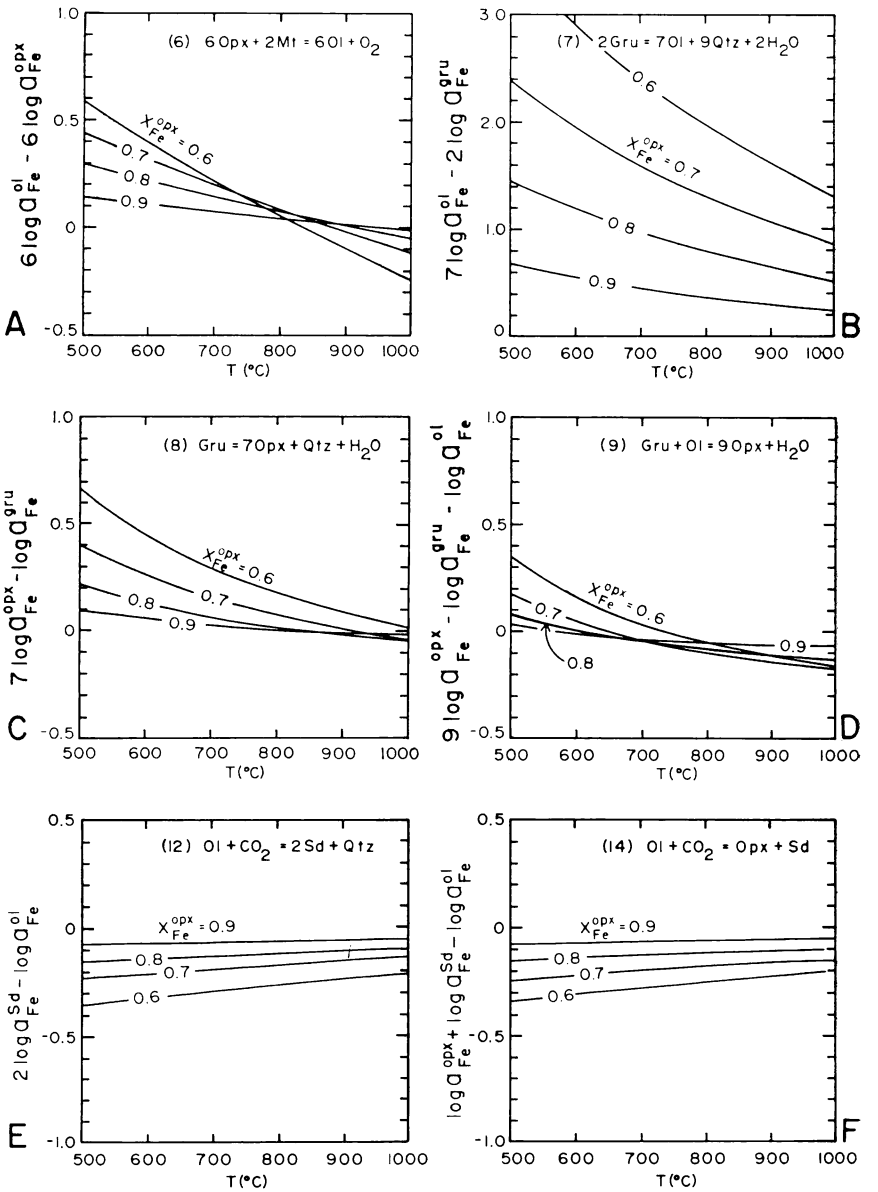

Fig. 2. Activity-temperature relations as a function of X_{Fe}^{opx} for representative metamorphic reactions. Compositions of coexisting minerals were taken from figure 3 in Miyano and Klein (1983), from data in Fonarev, Korolkov, and Dokina (1979), and from this study.

TABLE 1

Metamorphic reactions used in the text

(1) 3 grunerite + 3.5 O_2 = 7 magnetite + 24 quartz + 3 H_2O
(2) 2 grunerite + 6 magnetite = 16 olivine + 2 H_2O + 3 O_2
(3) 2 magnetite + 3 quartz = 3 olivine + O_2
(4) 3 grunerite + magnetite = 24 orthopyroxene + 3 H_2O + 0.5 O_2
(5) 2 magnetite + 6 quartz = 6 orthopyroxene + O_2
(6) 6 orthopyroxene + 2 magnetite = 6 olivine + O_2
(7) 2 grunerite = 7 olivine + 9 quartz + 2 H_2O
(8) grunerite = 7 orthopyroxene + quartz + H_2O
(9) grunerite + olivine = 9 orthopyroxene + H_2O
(10) olivine + quartz = 2 orthopyroxene
(11) grunerite + 7 CO_2 = 7 siderite + 8 quartz + H_2O
(12) olivine + 2 CO_2 = 2 siderite + quartz
(13) orthopyroxene + CO_2 = siderite + quartz
(14) olivine + CO_2 = orthopyroxene + siderite
(15) grunerite + 9 siderite = 8 olivine + 9 CO_2 + H_2O
(16) grunerite + siderite = 8 orthopyroxene + CO_2 + H_2O

grunerite $(Fe,Mg)_7Si_8O_{22}(OH)_2$, orthopyroxene $(Fe,Mg)SiO_3$, olivine $(Fe,Mg)_2SiO_4$, siderite $(Fe,Mg)CO_3$

Mineral abbreviations used in illustrations:
Fa = fayalite, Fs = ferrosilite, Gra = graphite, Gru = grunerite, Hm = hematite, Mt = magnetite, Ol = olivine, Opx = orthopyroxene, Qtz = quartz, Sd = siderite

tions for representative metamorphic reactions in table 1 as a function of X_{Fe}^{opx} on the basis of compositional relations of coexisting minerals. These relations will be used for an estimation of all phase equilibria involving solid solutions in the subsequent discussion.

COMPOSITIONS OF COEXISTING MINERAL PAIRS

The detailed compositional relations of Fe-rich olivine, orthopyroxene, grunerite, and siderite are essential to an evaluation of the high-temperature and pressure phase equilibria in the system Fe–Mg–Si–C–O–H. Figure 3 shows the compositional relations of Fe-rich olivine and orthopyroxene from various natural occurrences and experiments. These relations are a function of the equilibrium of Fe-Mg exchange as expressed in reaction A:

$$1/2Mg_2SiO_4 + FeSiO_3 = 1/2Fe_2SiO_4 + MgSiO_3 \qquad (A)$$

The Gibbs free energy change of reaction (A) has been estimated experimentally and theoretically by many workers (Matsumoto, 1971; Matsui and Nishizawa, 1974; Navrotsky, 1978; Sack, 1980; Fonarev, 1981a; Saxena, 1982). The estimated free energy values, however, differ considerably from one another (see fig. 4) and are inconsistent with Fe-Mg exchange data on coexisting Fe-rich olivine and orthopyroxene from natural assemblages and experiments. Sack (1980) found that the apparent equilibrium constant for Fe-Mg exchange between orthopyroxene and olivine could be used as a geothermometer. The present study estimates the Gibbs free energy change of reaction (A) on the basis of recent studies on orthopyrox-

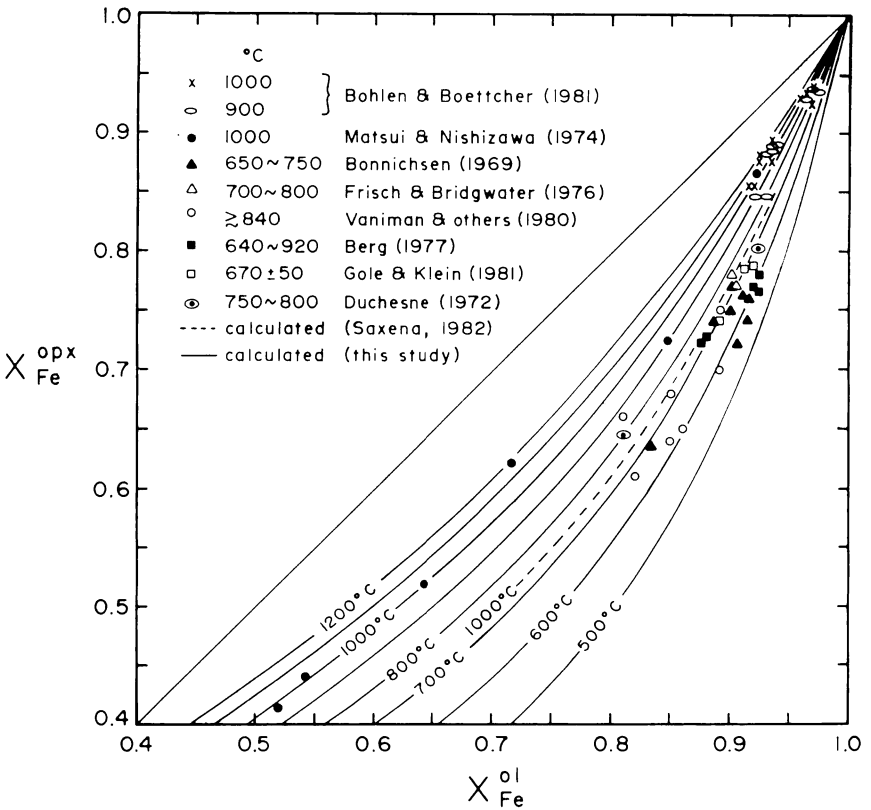

Fig. 3. X_{Fe}^{opx}–X_{Fe}^{ol} distribution isotherms in coexisting orthopyroxene and olivine. Solid isotherms were calculated in this study (see text); dashed from Saxena (1982).

ene by Chatillon-Colinet and others (1983) and on olivine by Wood and Kleppa (1981), using the experimental data of Bohlen and Boettcher (1981) for reaction (B):

$$\text{olivine} + \text{quartz} = 2\ \text{orthopyroxene} \qquad \text{(B)}$$

At equilibrium, the Gibbs free energy change $\Delta G_r(T_e,P_e)$ of reaction (B) can be expressed as: $\Delta G_r(T_e,P_e) = 0$, then

$$\Delta G^\circ{}_r(T_e) + \int_1^{Pe} \Delta V(T_e,P_e)dp = -RT\ln \frac{(a_{Fe}^{opx})^2}{a_{Fe}^{ol}} = -RT\ln \frac{(X_{Fe}^{opx})^2}{(X_{Fe}^{ol} \cdot \gamma_{Fe}^{ol})^2} \qquad (2)$$

where T_e and P_e are equilibrium temperature and pressure, respectively, from Bohlen and Boettcher (1981). $\Delta G^\circ{}_r(T_e)$ and $\Delta V(T_e,P_e)$ are standard Gibbs free energy change and volume change of reaction (B) for pure phases at T_e and P_e, respectively. They are evaluated from Miyano and Klein (1983). Solving eq (2) simultaneously with eq (1), X_{Fe}^{ol} in olivine

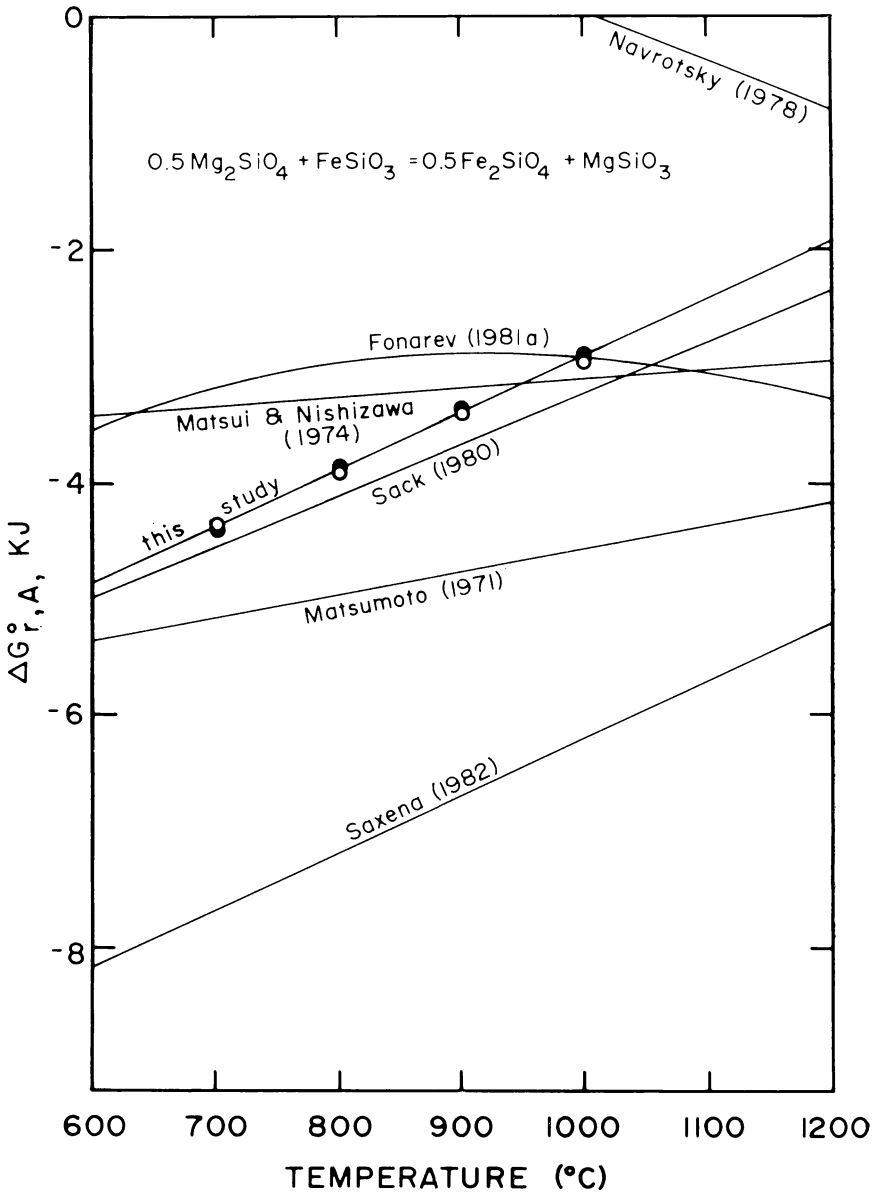

Fig. 4. Standard Gibbs free energy change for Fe–Mg exchange reaction of olivine and orthopyroxene. ○ and ●: calculated from experimental data of Bohlen and Boettcher (1981) at $X_{Fe}^{opx} = 0.9$ and 0.95, respectively, using eq (3).

coexisting with orthopyroxene at a given X_{Fe}^{opx} can be calculated, resulting in an apparent equilibrium constant ($K_D^{ol\text{-}opx}$) of Fe-Mg exchange in reaction (A). The Gibbs free energy change of reaction (A) $\Delta G°_{r,A}$ is therefore expressed as:

$$\Delta G°_{r,A} = -RT \ln \left[K_D^{ol\text{-}opx} \cdot \frac{\gamma_{Fe}^{ol}}{\gamma_{Mg}^{ol}} \right] \quad (3)$$

where $K_D^{ol\text{-}opx}$ denotes $(X_{Mg}^{opx} \cdot X_{Fe}^{ol})/(X_{Fe}^{opx} \cdot X_{Mg}^{ol})$. The estimated $\Delta G°_{r,A}$ values were normalized by linear regression ($\Delta G°_{r,A} = -9174 + 4.92\ T$ in Joul) and are illustrated in figure 4; they are somewhat larger than those of Sack (1980). Analogous to Saxena (1982), isotherms of compositional relations of coexisting olivine and orthopyroxene can be obtained from eqs (1) and (3) (fig. 3). Experimental data below 800°C were omitted from figure 3 because of large compositional variability. The isotherms in figure 3 are in good agreement with $X_{Fe}^{ol} - X_{Fe}^{opx}$ relations in coexisting pairs from natural assemblages and experiments; orthopyroxene occurs at temperatures above 550°C in natural assemblages. Temperatures for samples quoted by Vaniman, Papike, and Labotka (1980) and Bonnichsen (1975) range from 860° to 590°C and from 730° to 570°C, respectively. Probably these large temperature ranges are the result of a cooling process of igneous complexes in which orthopyroxene has retrogressively crystallized from olivine, as suggested by the authors.

Compositional relations of coexisting olivine and grunerite and coexisting orthopyroxene and grunerite were taken from high-grade metamorphosed iron-formations (Miyano and Klein, 1983) and experimental data (Fonarev, Korolkov, and Dokina, 1979). The relations were reevaluated on the basis of temperatures estimated from figure 3. As a result, the Fe-Mg distribution constant, $K_D^{ol\text{-}gru}$ between olivine and grunerite, may be estimated as follows:

$$\ln K_D^{ol\text{-}gru} = 2328.2/T(K) - 1.27 \quad (4)$$

where $K_D^{ol\text{-}gru} = (X_{Mg}^{gru} \cdot X_{Fe}^{ol})/(X_{Fe}^{gru} \cdot X_{Mg}^{ol})$. Combining eq (4) with $K_D^{ol\text{-}opx}$ (values in fig. 3), compositional relations of coexisting orthopyroxene, olivine, and grunerite can be predicted. For these coexisting silicates, estimated values of X_{Fe}^{opx} and X_{Fe}^{gru} at 700°C and given X_{Fe}^{ol} correlate well with assemblages 1A, 1B, and 4C of Gole and Klein (1981), where values in parentheses represent calculated values:

	sample 1A		sample 1B		sample 4C	
X_{Fe}^{ol}	0.890	(0.890)	0.917	(0.917)	0.912	(0.912)
X_{Fe}^{opx}	0.739	(0.740)	0.787	(0.793)	0.784	(0.783)
X_{Fe}^{gru}	0.725	(0.725)	0.765	(0.765)	0.769	(0.771)

Because compositional data on coexisting siderite and grunerite or siderite and orthopyroxene are limited, we used the data from Butler (1969) and Klein (1978). Generally, X_{Fe}^{sd} is greater than X_{Fe}^{gru} and slightly smaller than X_{Fe}^{opx} at 600° to 750°C.

UPPER PRESSURE STABILITY LIMIT OF OLIVINE

X_{Fe}^{opx} and X_{Fe}^{ol} of coexisting olivine and orthopyroxene in iron-rich rocks, as well as iron-formations, are restricted within the ranges from 0.6 to 0.8 and from 0.8 to 0.93, respectively (fig. 3). This implies that orthopyroxene with $X_{Fe}^{opx} > 0.8$, and < 0.6 is not likely to be associated with olivine. Using the assemblage Ol–Opx–Qtz, the upper pressure stability limit of olivine, above 800°C, can be determined from the experimental data of Bohlen and Boettcher (1981). The limit below 800°C can be calculated, in the presence of magnetite, by using the compositional relations of figure 3 and the solid solution models for olivine and orthopyroxene, referred to earlier. The calculated results of equilibria (3), (5), and (6), are expressed in P-log $f(O_2)$ space, at a fixed temperature (600°, 700°, 800°C) in figure 5,A through C. In these diagrams, curves are given for $X_{Fe}^{opx} = 0.6$ and 0.8. The stability field of orthopyroxene can expand in the direction of higher oxygen fugacity as well as lower pressure, with decreasing X_{Fe}^{opx}. With decreasing pressure, two curves (for Ol–Opx–Mt and Opx–Qtz–Mt for $X_{Fe}^{opx} = 0.8$) meet at points A (600°C), B (700°C), and C (800°C) at the termination point of the Opx field. At pressures below these points, $f(O_2)$ is buffered by Ol–Qtz–Mt. The T-$f(O_2)$ conditions for high-grade metamorphosed iron-formations can be divided into three types: (1) olivine-free, (2) olivine- and quartz-bearing, and (3) olivine-bearing and quartz-free assemblages in the presence of magnetite (Miyano and Klein, 1983). The possible metamorphic P-$f(O_2)$ conditions for most iron-formations are therefore constrained by three curves: Opx($X_{Fe}^{opx} = 0.8$)–Qtz–Mt, Opx($X_{Fe}^{opx} = 0.6$)–Qtz–Mt, and Ol–Qtz–Mt, as shown by the shaded regions in figure 5, at a fixed temperature. Accordingly, the invariant points A, B, and C represent the upper pressure stability limit of olivine. Although olivine may be stable above these points, in the absence of quartz, it would be metastable in iron-formations in which quartz is generally an abundant constituent. Vaniman, Papike, and Labotka (1980) reported several assemblages of Opx–Ol–Mt without quartz from the Stillwater iron-formations, where metamorphic conditions were $P \gtrsim 2$ kb, $T \gtrsim 840$°C, $0.6 < X_{Fe}^{opx} < 0.75$, and $0.8 < X_{Fe}^{ol} < 0.9$. Although some of the orthopyroxenes in the assemblages are retrograde, the P-$f(O_2)$ conditions of the iron-formations can be located within the shaded regions of figure 5,A to C but below points A, B, and C. This implies that $f(O_2)$ in high-grade metamorphic iron-formations is generally greater than that defined by the QFM buffer ($X_{Fe}^{ol} = 1.0$, dot-dashed curve (3) in fig. 5,A-C). The Opx–Ol–Mt assemblage is rare in iron-formations and will probably occur only under very dry conditions, which can be attained at very high temperatures (> 800°C). Retrogressive orthopyroxene appears to form along an oxygen-buffered path defined by the initial assemblage of Opx–Ol–Mt at about 840°C (see Miyano and Klein, 1983).

The upper pressure limit of olivine is consistent with the relatively low-pressure occurrences of olivine in regionally metamorphosed (Haase, 1982a; Gole and Klein, 1981) and contact metamorphosed iron-formations (French, 1968; Bonnichsen, 1969, 1975; Morey and others, 1972; Simmons, Lindsley, and Papike, 1974; Floran and Papike, 1978).

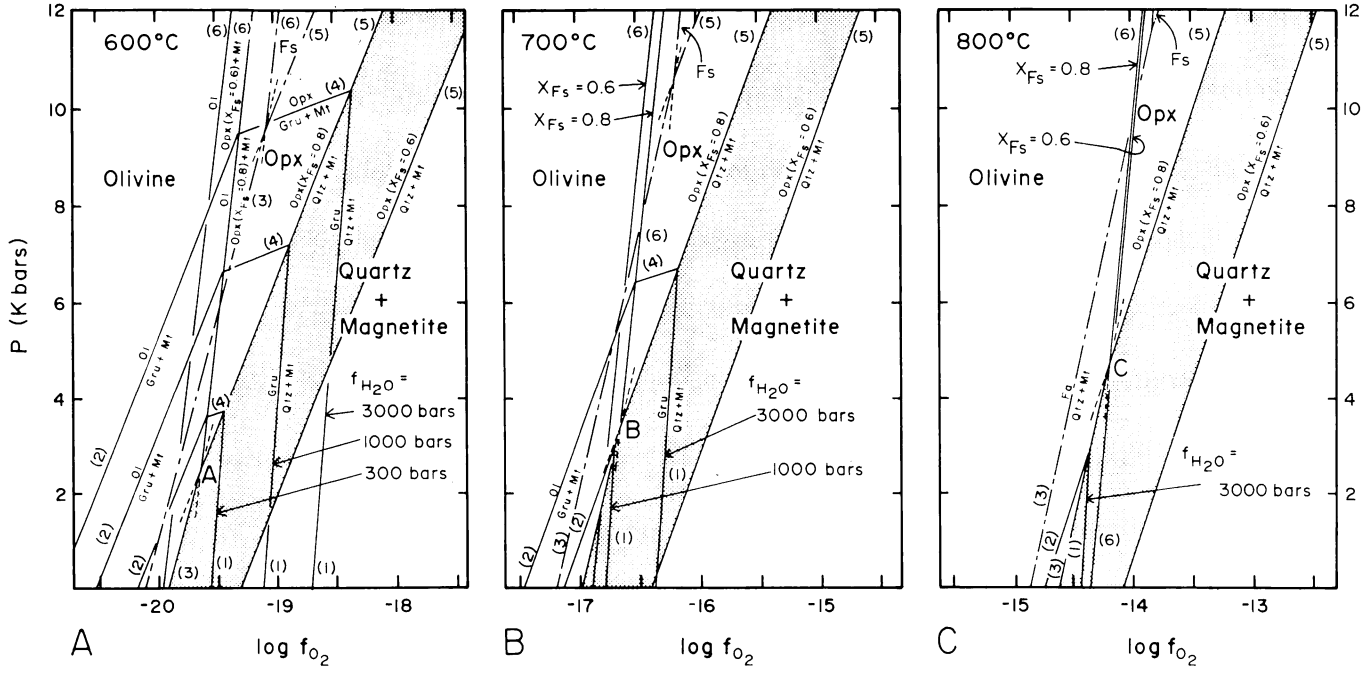

Fig. 5. P-log f(O_2) diagram showing the metamorphic conditions for iron-formations and the upper pressure limit of olivine. (A) at 600°C, (B) at 700°C, and (C) at 800°C. See table 1 for abbreviations. $X_{Fs} = X_{Fe}^{opx}$. Number in parentheses denotes the number of the reaction given in table 1. Dot-dashed curves (3), (5), and (6) are drawn for the pure endmembers of fayalite and ferrosilite. The shaded area, bordered by curves (3) and (5) (at $X_{Fe}^{opx} = 0.8$ and 0.6), reflects the most likely P-f(O_2) conditions attained during high-grade metamorphism of iron-formations. Points A, B, and C are equivalent to the upper pressure limit of olivine + quartz at 600°, 700°, and 800°C, respectively. The stability of grunerite was calculated at fixed f(H_2O) on the basis of the thermodynamic data of this study.

STABILITY FIELDS OF SIDERITE AND GRUNERITE

Siderite stability in high-grade metamorphism.—As noted earlier, the mineral assemblages in high-grade metamorphosed iron-formations may be divided into three types on the basis of the T-f(O_2) conditions; siderite is found only in type 1 (type C in this study) and generally does not coexist with olivine. One exception has been reported by Floran and Papike (1978) from the contact-metamorphic Gunflint Iron Formation, where siderite occurs as a relict coexisting with fayalite in an assemblage of type 2 (type A in this study). Assemblages involving siderite, such as Qtz–Sd–Mt, Opx–Gru–Sd–Qtz–Mt, Opx–Qtz–Sd–Mt, and Qtz–Sd–Opx–Gru–Gra have been described from high-grade metamorphosed iron-formations in the Labrador Trough, Canada (Butler, 1969; Klein, 1978). The estimated P-T conditions of metamorphism are above 600°C and about 6 kb for Butler's assemblages (Klein, 1983) and 700° to 750°C and 10 to 11 kb for Klein's (Klein, 1978). X_{Fe}^{Sd} of siderite in these iron-formations ranges from 0.63 to 0.78 (Butler, 1969; Klein, 1978 and unpublished data).

The stability relations of siderite have been studied experimentally in the system Fe–C–O (French, 1971; Weidner, 1972). Siderite is stable up to 640°C at 6 kb and up to 740°C at 10 kb, as based on equilibria in the assemblage siderite–magnetite–carbon–vapor (Weidner, 1972). This stability range is not consistent with that calculated from data by Robie, Hemingway, and Fisher (1978) or Helgeson and others (1978). Robie, Haselton, and Hemingway (1984) measured the standard molal heat capacity and entropy of siderite and obtained $\Delta G°_{f,298}$ of −680.0 to −685.5 KJ mol^{-1} for siderite. The calculated stability relations of siderite, based on −685.5 KJ mol^{-1}, are in good agreement with French's experimental equilibria for assemblages siderite–hematite–magnetite–vapor and siderite–magnetite–graphite–vapor only at 2 kb and are comparable with Weidner's results (see fig. 6). However, French's data at 0.5 and 1 kb are not consistent with the calculated ones (fig. 6). Considering experiments on the assemblages at 1 bar total pressure (Seguin, 1971), siderite and hematite decompose to form magnetite at 285° ± 8°C and siderite to form magnetite and graphite at 388° ± 10°C, which is compatible with curves (A) and (B) in figure 6, respectively. Siderite in French's experiments at 0.5 and 1 kb may have been metastable.

Using the thermodynamic data of Robie, Haselton, and Fisher (1984) for siderite, of Shmulovich and Shmonov (1975) for CO_2 (also see Perchuk (1977), and Holland (1981) for f(CO_2)), the P-T conditions for siderite-bearing assemblages can be estimated on the basis of the following reactions (12), (13), and (14) (figs. 6 and 13):

(12) olivine + $2CO_2$ = 2 siderite + quartz,

(13) orthopyroxene + CO_2 = siderite + quartz,

and

(14) olivine + CO_2 = siderite + orthopyroxene.

If X_{Fe}^{ol} and X_{Fe}^{opx} are close or equal to unity, the second and third reactions will not occur at pressures below about 10 kb and at temperatures

above 600°C (Bohlen and Boettcher, 1981). The univariant curves (12), (13), and (14) shift toward the high-temperature side with decreasing X_{Fe}^{sd} (or X_{Fe}^{ol} or X_{Fe}^{opx}). Because X_{Fe}^{opx} for orthopyroxene coexisting with siderite is greater than 0.6 to 0.7, curve (13) (see fig. 13,A and B) shows the maximum temperature (at $P_s = P(CO_2)$) for siderite stability in iron-formations. The P-T conditions of Butler (1969) and Klein (1978) lie on this

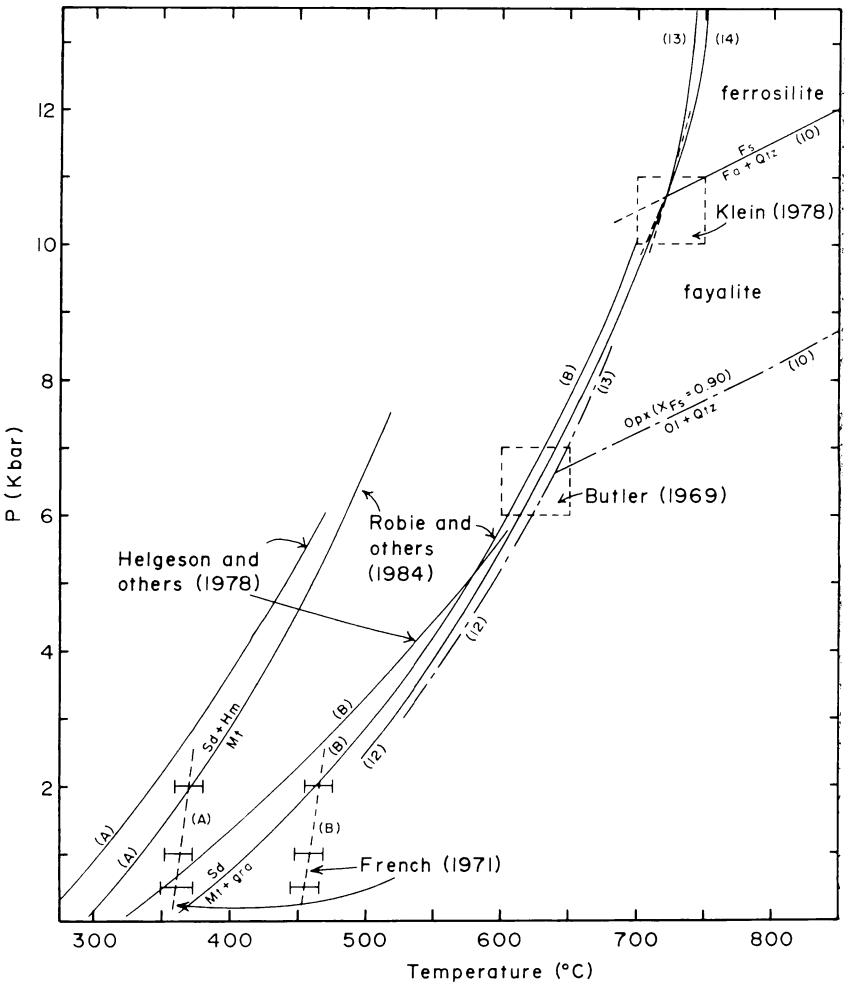

Fig. 6. Calculated P-T diagram showing the stability of siderite at Ps = $P_{total\ fluid}$. Thermodynamic properties for siderite from Robie, Haselton, and Hemingway (1984) are a better fit to experiments (reactions A and B) of French (1971) at 2 kb, and probably of Weidner (1972) above 6 kb, than those of Helgeson and others (1978) (see text). Solid curves (10), (12), and (13) are for the pure phases siderite, fayalite, and ferrosilite, respectively. Dot-dashed curves (10), (12), and (13) are drawn at X_{Fs} (= X_{Fe}^{opx}) = 0.90. P-T conditions for siderite-bearing iron-formations are shown in boxes. (A) siderite + hematite = magnetite + vapor. (B) siderite = magnetite + graphite + vapor.

maximum temperature limit for siderite. Such siderite-bearing iron-formations have undergone high-grade metamorphism with an apparent geothermal gradient of less than about 100°C/kb. The assemblages siderite–olivine and siderite–orthopyroxene are not stable on the high-temperature side of curves (12) and (13), where the geothermal gradient is greater than 100°C/kb (fig. 6). This is consistent with the general absence of such assemblages in many high-grade metamorphic iron-formations (French, 1968; Bonnichsen, 1969, 1975; Simmons, Lindsley, and Papike, 1974; Immega and Klein, 1976; Floran and Papike, 1978; Dahl, 1979; Vaniman, Papike, and Labotka, 1980; Gole and Klein, 1981). The assemblage defined by reaction (14) cannot occur in the presence of magnetite at pressures higher than the upper pressure limit of olivine, as already mentioned. If retrograde metamorphism follows a P-T path from siderite-free to siderite-bearing assemblages (thereby crossing curves (12) and (13)), secondary siderite, as proposed by Anovitz and Essene (1986), could form provided $P(CO_2)$ is high enough.

Siderite-graphite stability.—Butler (1969) reports the assemblages Sd–Qtz–Opx($X_{Fe}^{opx} = 0.73$)–Gru–Gra and Qtz–Opx($0.61 \leqslant X_{Fe}^{opx} \leqslant 0.73$)–Gra ± Gru ± Mt from the Wabush Iron Formation in the southern part of the Labrador Trough. Because the first assemblage includes no magnetite, the estimated $f(O_2)$ may be expected to be lower than the QOM (Qtz–Opx–Mt) buffer; furthermore, reduced gas species may have played a part. From such an assemblage, we may deduce the following oxygen-buffer reaction:

$$\text{siderite} + \text{quartz} = \text{orthopyroxene} + \text{graphite} + O_2 .$$

The phase relations of French (1971) can be recalculated at 6 kb on the basis of the thermodynamic properties determined in this study (fig. 7). The curve of the above reaction lies within the stability field of siderite + graphite and between the QOM and QFM buffers. As a result, the abundance of reduced species such as CH_4 and H_2 is less than that estimated from the QFM buffer, that is, < 0.005 at 6 kb ($=P_f$) and < 0.01 at 3 kb ($=P_f$). Butler's second assemblage (noted above) involves magnetite in places. It is thus possible that $f(O_2)$ is close or equal to that defined by the QOM buffer. Therefore, the fluid compositions for graphite-bearing assemblages may be computed in a manner similar to those in the H_2O–CO_2 mixed-volatile region, on the basis of equilibria for assemblages Opx–Gru–Qtz–Sd or Opx–Gru–Qtz.

Because graphite-bearing assemblages reported in the literature are scarce in high-grade metamorphic iron-formations, the phase relations involving graphite will not be treated in this study. Such phase relations and their significance have been evaluated by Burt (1972) and Frost (1979a,b).

Grunerite stability.—The stability of pure grunerite was experimentally determined by Forbes (1977) and Mel'nik and Radchuk (1977) on the basis of the reaction grunerite = fayalite + quartz + H_2O, using various buffers. Although neither set of experiments was reversed, the P-T

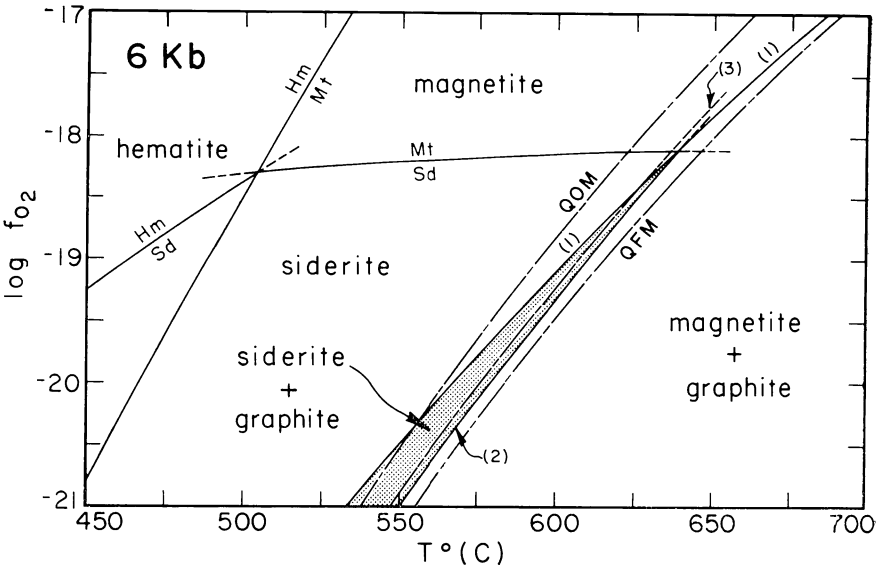

Fig. 7. log $f(O_2)$-T diagram showing the stability field of siderite + graphite at $X_{Fe}^{opx} = 0.73$ and $P_f = 6$ kb. P_f is essentially equal to $P(CO_2)$ above the QFM buffer. Assemblage Sd–Gra–Opx–Qtz (Butler, 1969) is shown by dashed curve (3) within the field of siderite + graphite (shaded). QOM: Qtz–Opx ($X_{Fe}^{opx} = 0.73$)-Mt, QFM = Qtz–Fa ($X_{Fe}^{ol} = 1.0$)-Mt. (1): $C + O_2 = CO_2$, (2): Sd = Mt + C + O_2, (3): Sd + Qtz = Opx + C + O_2.

conditions of Mel'nik and Radchuk (1977) are in good agreement with those of Forbes (1977) at the WM buffer (fig. 8). The conditions lie between the estimated stabilities of Fonarev (1981b) and Miyano and Klein (1983). The stability field calculated by Fonarev was based on experiments using an Fe-Mg cummingtonite (Fonarev, Korolkov, and Dokina, 1976, 1979; Fonarev and Korolkov, 1980) and applying an asymmetric solution model. Because, as mentioned above, his results show a larger deviation from ideality for grunerite than those of this study, the P-T conditions determined by Fonarev could shift to higher temperatures (by 30°-50°C) approaching those of Forbes (1977, WM buffer) and Mel'nik and Radchuk (1977) when our solution model is used. Mel'nik and Radchuk gave four equilibrium P-T brackets for reaction (7), (580°C, 0.5 kb), (609°C, 1.0 kb), (636°C, 2.0 kb), and (650°C, 3.0 kb), with temperature uncertainties of ± 10°C. Using these brackets, they estimated $S°_{298}$ and $\Delta G°_{f,298}$ as 810.9 joul mol^{-1} deg^{-1} and −8934.5 Kjoul mol^{-1} deg^{-1}, respectively, assuming $\Delta Cp = 0$. Their entropy value is much larger by 89 joul mol^{-1} than the predicted value 721.8 joul mol^{-1} of Miyano and Klein (1983). Using the measured heat capacity of grunerite from Bennington, Ferrante, and Stuve (1978, adjusted for pure grunerite by Miyano and Klein, 1983), we calculate the difference between the entropy values of grunerite at experimental temperature and 25°C to be 82 joul mol^{-1} at 580°C and 90 joul mol^{-1}

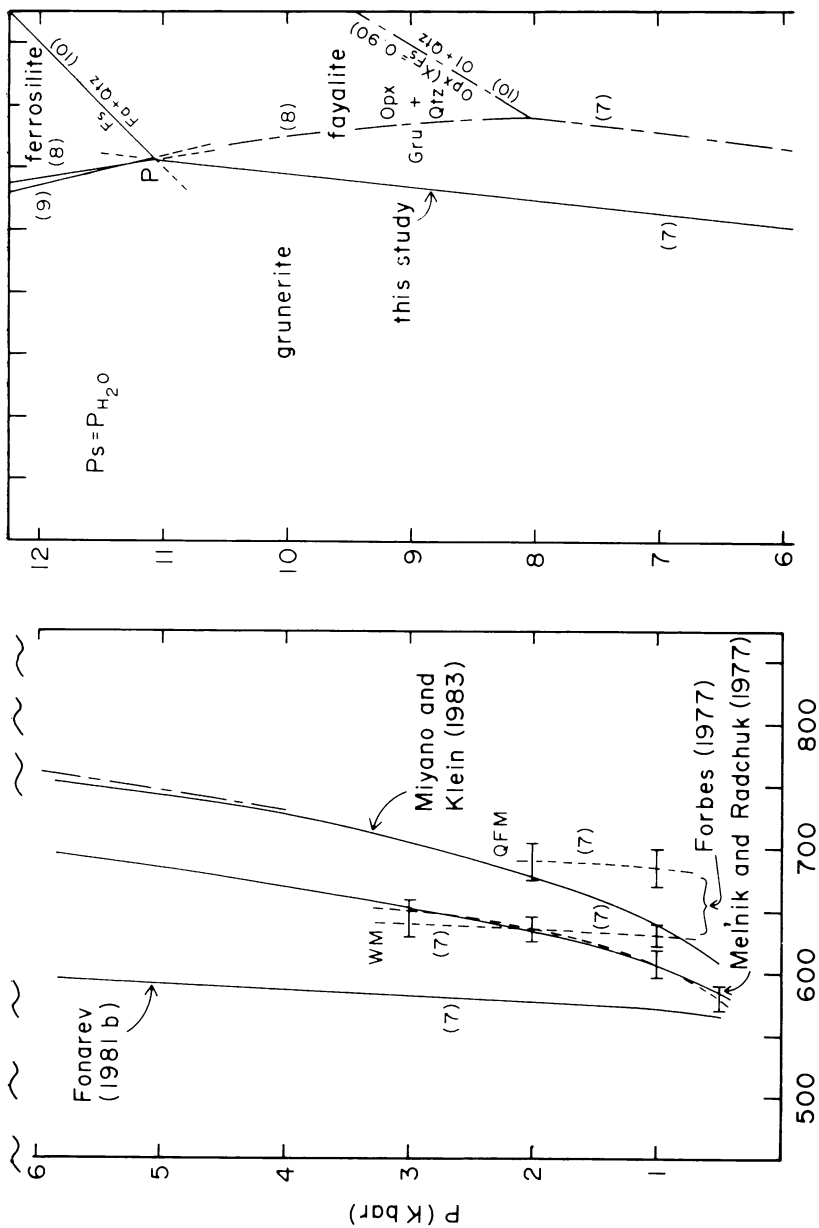

Fig. 8. Calculated and experimental P-T conditions for equilibria of grunerite = fayalite + quartz + water at $P_s = P(H_2O)$. Dashed curves represent experiments (Forbes, 1977; Melʹnik and Radchuk, 1977). Solid curve (7), calculated from thermodynamic properties for grunerite in this study, lies between the P-T conditions of Fonarev (1981b) and Miyano and Klein (1983). The assemblage of the pure phases grunerite, ferrosilite, and fayalite is shown at invariant point **P**. Dot-dashed curves (7), (8), and (10) are drawn at $X_{Fe}(= X_{Fe}^{opx}) = 0.90$.

at 650°C. This difference is analogous to that between the value of Mel'nik and Radchuk (1977) and the one predicted by Miyano and Klein (1983). The assumptions made by Mel'nik and Radchuk (1977) seem therefore not to be valid in this case. Accordingly we recalculated $S°_{298}$, $\Delta H°_{f,298}$, and $\Delta G°_{f,298}$ of grunerite to be 714.6 ± 20 joul mol^{-1} deg^{-1}, −9626.5 ± 19 Kjoul mol^{-1}, and −8964.8 ± 19.9 Kjoul mol^{-1}, respectively, using heat capacity power functions of all materials in reaction (7) from Robie, Hemingway, and Fisher (1978) and Miyano and Klein (1983). Uncertainty estimates are those described by Fisher and Zen (1971) and Zen (1972, 1977). The recalculated entropy value is in good agreement with the predicted one of Miyano and Klein. The $S°_{298}$ and $\Delta G°_{f,298}$ values are comparable with 721.8 joul mol^{-1} deg^{-1} and −8966.8 (maximum) Kjoul mol^{-1} of Miyano and Klein (1983) and 637.6 joul mol^{-1} deg^{-1} and −8980.5 Kjoul mol^{-1} of Fonarev (1981b), respectively. Because grunerite-bearing reactions (8) and (9) have negative slopes (in T-P space, above 11 kb) adjoining the ferrosilite stability field, the maximum temperature stability for pure grunerite is approx 760°C (see fig. 8).

Using the stability data for siderite and grunerite mentioned above, phase relations in the system Fe–Si–C–O–H for siderite, grunerite, fayalite, and quartz can be constructed in T-X(CO_2) space. Figure 9 shows these phase relations at 1 and 3 kb, using a non-ideal mixing model for CO_2 and H_2O. Because ferrosilite with $X_{Fe}^{opx} \approx 1.0$ is not stable below 10 kb and above 600°C (fig. 8), the phase relations in figure 9 do not involve ferrosilite.

The effect of additional Mg in the silicates and siderite is evaluated on the basis of the activity-temperature relations given in figure 2. Generally, the equilibrium curves shift toward higher temperature with increasing Mg contents, as shown in figures 6 and 8 for T-P space and figure 9 for T-X(CO_2) space. However, the phase relations for iron-formations, with more magnesian minerals, cannot be fully evaluated in these diagrams. They are discussed below.

PHASE EQUILIBRIA IN THE SYSTEM Fe–Mg–Si–C–O–H

The important gas species in high-grade metamorphic rocks occur in the system C–H–O–S and are constrained by the coexistence of silicates, carbonates, and sulfides (for example, Eugster and Skippen, 1967; Eugster, 1977; Ohmoto and Kerrick, 1977; Holloway, 1981; Ferry and Burt, 1982). The major gas species in this system are H_2, CO_2, CH_4, CO, H_2S, SO_2, et cetera. Sulfur-bearing species may, however, be ignored because, even in relatively sulfur-rich fluids, H_2S will be orders of magnitude less abundant than H_2O or CO_2 (for example, Ohmoto and Kerrick, 1977). In the following treatment, fluids are limited to gas species in the system C–H–O.

The fluid behavior in the system C–H–O was evaluated by Holloway (1977, 1981) and Frost (1979b) at high temperatures and pressures with a non-ideal mixing model using a modified Redlich and Kwong (MRK) equation. Frost (1979a,b) showed that the fluid coexisting with an iron-formation containing magnetite + quartz is essentially a binary H_2O-CO_2 mixture. Although his calculations for an Mg-free system should be some-

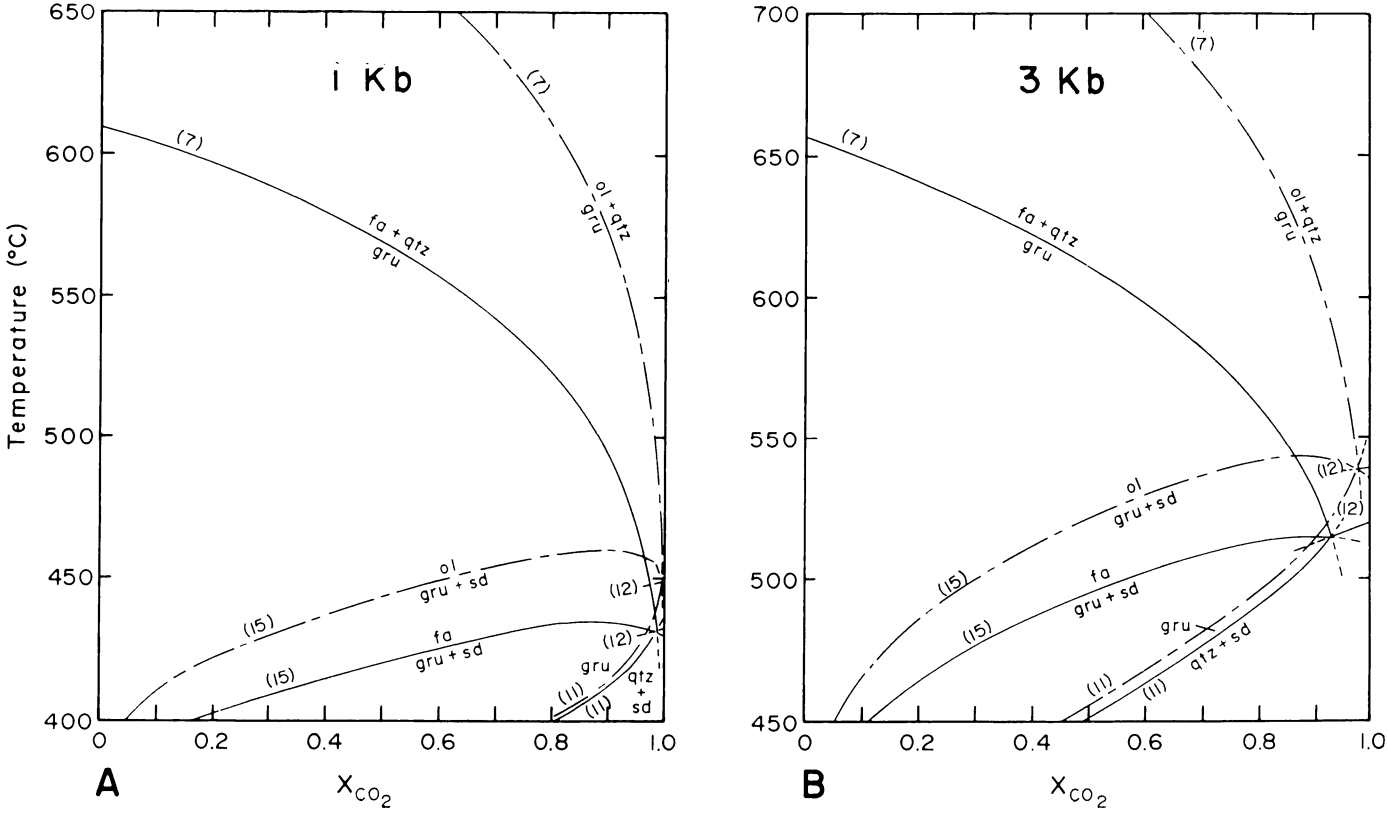

Fig. 9. T-X(CO_2) diagrams showing phase relations of fayalite, grunerite, siderite, and quartz at $P_s = P(H_2O) + P(CO_2)$. 9-A: 1 kb at $X_{Fe}^{ol} = 1.0$ (solid lines) and $X_{Fe}^{ol} = 0.9$ (dot-dashed). 9-B: 3 kb at $X_{Fe}^{ol} = 1.0$ (solid lines) and $X_{Fe}^{ol} = 0.9$ (dot-dashed). The phase relations in the figures show those of type A which excludes orthopyroxene.

what adjusted to account for the non-ideality of the fluid phase (see also Flowers, 1979), our calculations indicate that the addition of Mg acts only to decrease the abundance of the reduced species. They also show that the mole fraction of reduced species such as CH_4 and H_2 coexisting with graphite is less than 0.02 at the QFM buffer at 1 kb above 400°C and decreases with increasing pressure. Because the $f(O_2)$ for most of iron-formations is greater than that defined by the QFM buffer, the binary CO_2-H_2O mixture model of Frost (1979a,b) and Haase (1982b) is reasonable for the fluid during high-grade metamorphism of iron-formations.

Prior to any calculations of the equilibria in the system Fe–Mg–Si–C–O–H, the possible topology of the phase relations of mineral assemblages in iron-formations was assessed using Schreinemakers' method (Zen, 1966). The stability relations of olivine, orthopyroxene, grunerite, quartz, and siderite in T-P space are schematically shown at fixed $X(CO_2)$ and X_{Fe}^{opx} in figure 10. Because of compositional constraints on olivine ($X_{Fe}^{ol} > 0.8$) and orthopyroxene ($0.6 < X_{Fe}^{opx} < 0.8$) in most metamorphic iron-formations, orthopyroxene coexists with olivine at pressures below 2 to 5 kb above 550°C. The topology can therefore be divided into three types: (A) olivine-bearing and orthopyroxene-free (< 2-5 kb, > 400°C), (B) olivine- and orthopyroxene-bearing (< 2-5 kb, > 550°C), and (C) olivine-free and orthopyroxene-bearing (> 2-5 kb, > 550°C) assemblages. These types are equivalent to those shown in figure 10. Because orthopyroxene with $X_{Fe}^{opx} = 0.6$ to 0.8 is unlikely to coexist with olivine below 550°C, only type A is present below this temperature. Type A can persist to higher temperatures (>550°C) provided that X_{Fe}^{ol} is greater than 0.93 at pressures below 2 to 5 kb; here olivine is unlikely to coexist with orthopyroxene in iron-formations.

The phase relations for these three types (A, B, and C) in T-$X(CO_2)$ are shown in figures 11, A, B, and C, respectively, in which X_{Fe} is fixed. Because the upper stability limit of siderite, in the presence of quartz, is bordered by curves (12) and (13), siderite-bearing assemblages in T-$X(CO_2)$ space will be restricted to below these limits. Consequently siderite is absent from iron-formations of type A (>550°C) and type B. The phase relations for the assemblages in type A below 550°C are shown in figure 9 and the inset of figure 10.

Opx-free and Ol-bearing iron-formations equivalent to type A have been reported from the Negaunee Iron Formation (Haase, 1982a) and from high-grade portions of the Biwabik and Gunflint Iron Formations (Morey and others, 1972; Bonnichsen, 1975; Floran and Papike, 1978) excluding assemblages that are in the immediate contact zone of the Duluth Gabbro Complex. Type B, with olivine and orthopyroxene, is equivalent to several contact and regionally metamorphosed iron-formations (French, 1968; Bonnichsen, 1969, 1975; Simmons, Lindsley, and Papike, 1974; Floran and Papike, 1978; Vaniman, Papike, and Labotka, 1980; and Gole and Klein, 1981). Type C corresponds to regionally metamorphosed iron-formations (Klein, 1966, 1978; Chakraborty, 1966; Butler, 1969; Immega and Klein, 1976; and Dahl, 1979). The assemblage Opx–

Ol–Gru–Qtz is observed in several iron-formations (for example, Gundersen and Schwartz, 1962; French, 1968; Bonnichsen, 1969, 1975; Gole and Klein, 1981).

The phase relations in the system Fe–Mg–Si–C–O–H can be estimated quantitatively using the activity-temperature relations shown in figure 2

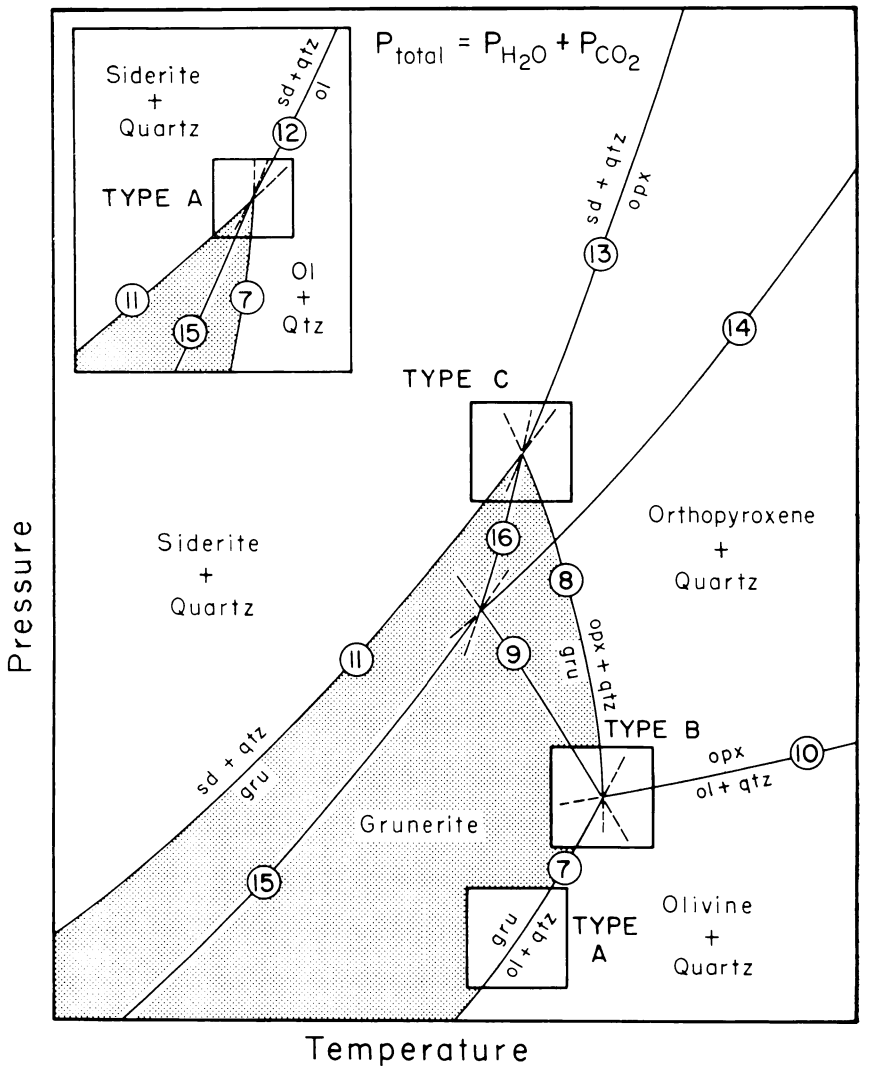

Fig. 10. Schematic P-T diagram showing phase relations of orthopyroxene, olivine, grunerite, quartz, and siderite at constant $X(CO_2)$ and X_{Fe}^{opx}. In iron-formation assemblages, the phase relations can be divided into three types: (A) Ol-bearing and Opx-free; (B) Ol- and Opx-bearing; and (C) Ol-free and Opx-bearing assemblages. These types are equivalent to those in figure 11. Siderite-bearing relations (type A) are shown in the inset and probably occur in medium-grade rocks ($< 550°C$).

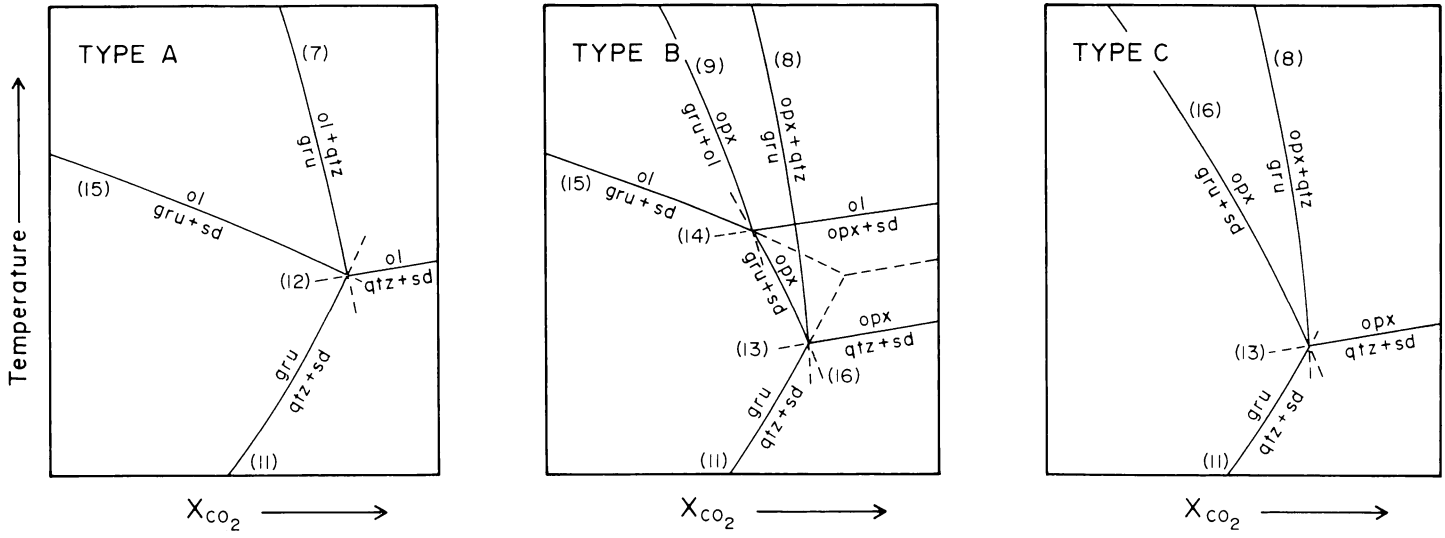

Fig. 11. Schematic T-X(CO_2) diagrams at fixed X_{Fe}^{opx} showing phase relations of orthopyroxene, olivine, grunerite, siderite, and quartz. Compare with figure 10. Because siderite is not stable at pressures of 2 to 5 kb above 600°C, the phase relations of type B cannot be fully represented for high-grade metamorphosed iron-formations. All the phase relations for type B appear to be possible in even more iron-rich rocks at higher pressure.

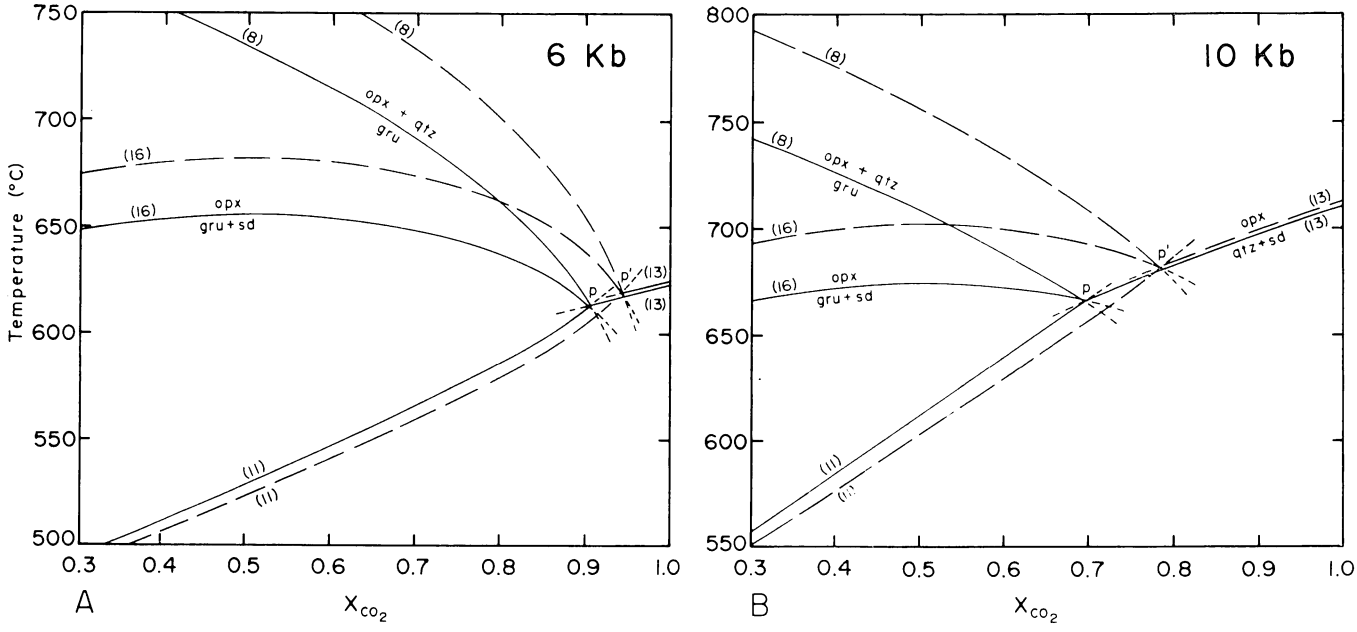

Fig. 12. Calculated T-X(CO_2) diagrams showing the phase relations for type C at $P_s = P_{H_2O} + P_{CO_2}$.
A. 6 kb at $X_{Fe}^{opx} = 0.6$ (dashed lines) and 0.8 (solid lines).
B. 10 kb at $X_{Fe}^{opx} = 0.6$ (dashed lines) and 0.8 (solid lines).

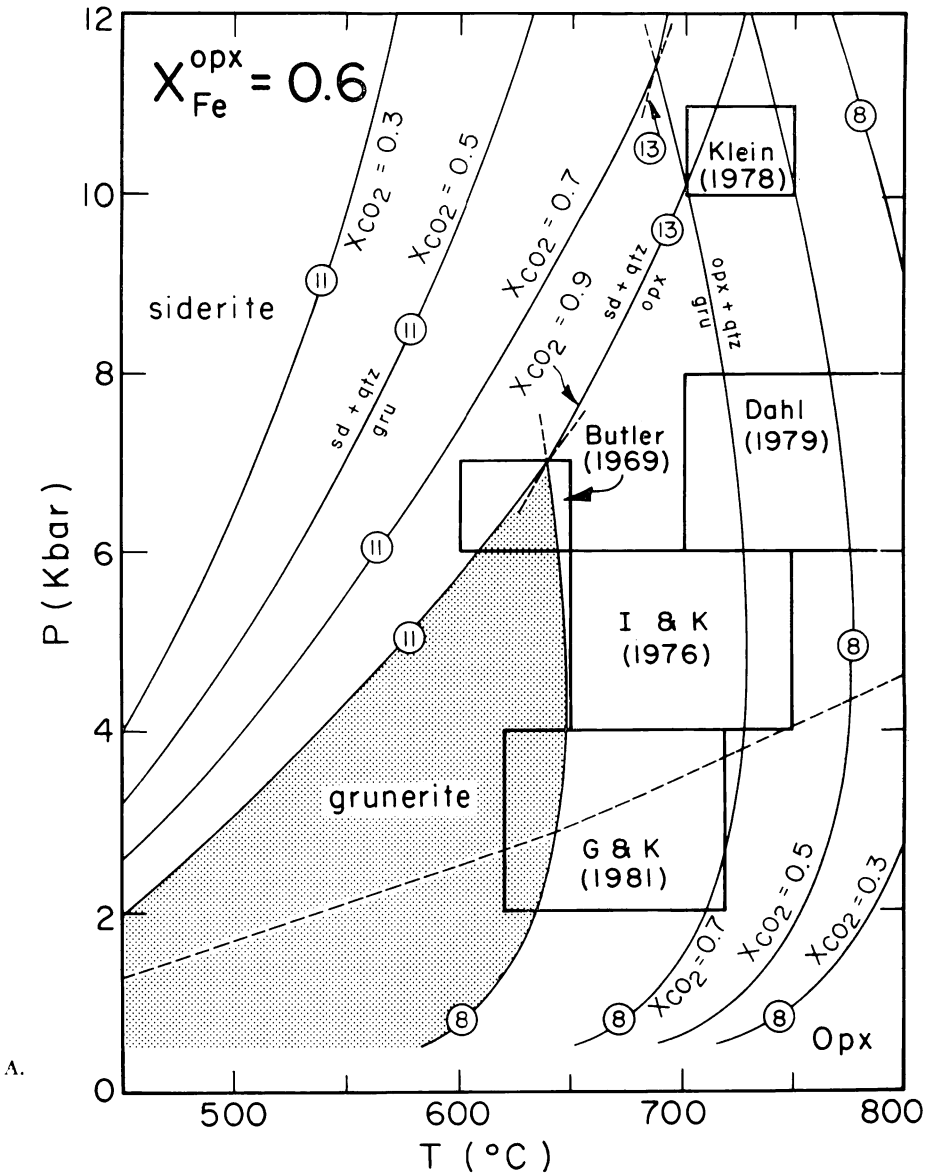

A.

Fig. 13. Calculated P-T diagrams showing phase relations of orthopyroxene, olivine, grunerite, quartz, and siderite at given X_{Fe}^{opx} and $X(CO_2)$ and at $P_s = P(H_2O) + P(CO_2)$.

(A) $X_{Fe}^{opx} = 0.6$. (B) $X_{Fe}^{opx} = 0.7$. (C) $X_{Fe}^{opx} = 0.8$. (C on p. 564.)

Topologies in the figures are the same as in figure 10, but they were constructed in the

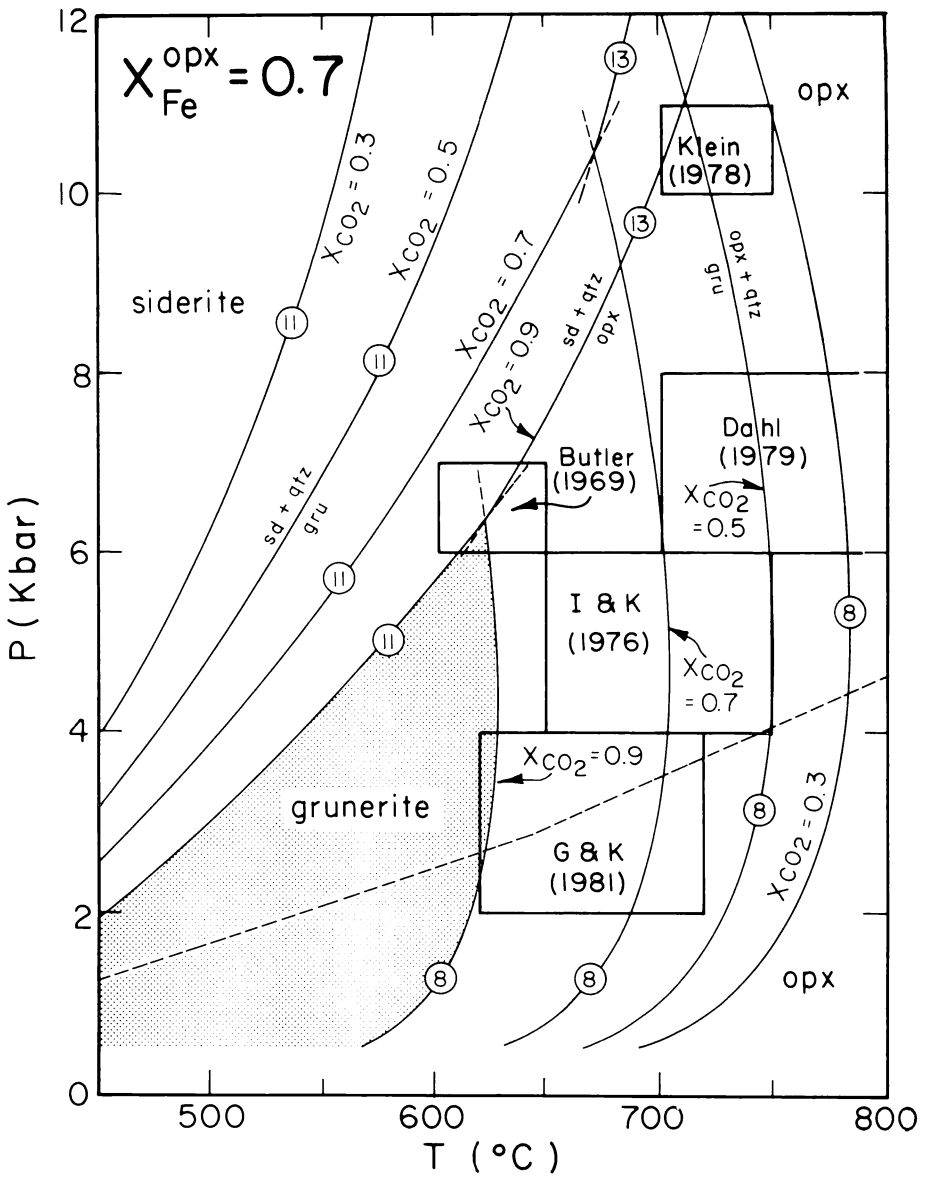

B.

presence of quartz, and therefore curve (9) is not shown. Dashed lines in (A) and (B), indicate the upper pressure limit (reaction 10) of olivine at $X_{Fe}^{opx} = 0.80$. Gole and Klein's (1981) data were adjusted according to new experimental data of Bohlen and Boettcher (1981). I & K: Immega and Klein (1976), G & K: Gole and Klein (1981). The grunerite field at $X(CO_2) = 0.9$ is shaded.

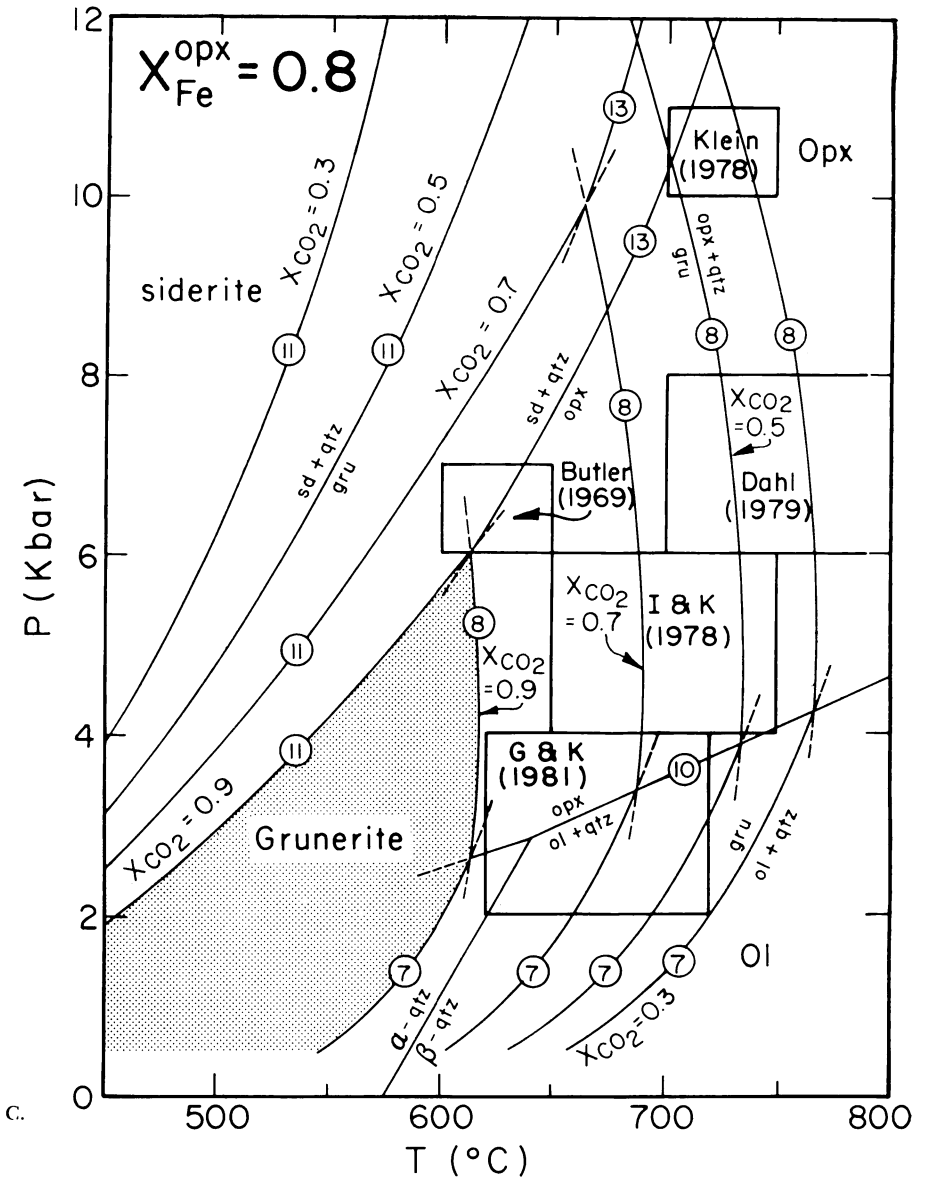

C.

and the thermodynamic properties mentioned earlier. The relations in T-X(CO_2) space were computed on the basis of the method outlined by Kerrick (1974) using a program N88BASIC-BINARY written by T. M. The activities of CO_2 and H_2O in the binary gas mixture were calculated using MRK equations (Holloway, 1977; Flowers, 1979; Kerrick and Jacobs, 1981). The results are illustrated in terms of T-X(CO_2) (figs. 9 and 12) and

for T-P conditions (fig. 13A, B, and C), where the effect of Mg substitution in the silicates and siderite is expressed as a function of X_{Fe}^{opx}. Although the topology of figure 13A, B, and C, is the same as that of figure 10, it was constructed in the presence of quartz at $P_s = P(H_2O) + P(CO_2)$, with $X(CO_2)$ ranging from 0.3 to 0.9. In figure 13, curves (7) (in fig. 13C) and (8) show major shifts as a function of varying both X_{Fe}^{opx} and $X(CO_2)$, but curves (11) and (13) are not sensitive to the variation of X_{Fe}^{opx}. Thus the stability field of grunerite expands to both low and high temperatures and high pressure with decreasing $X(CO_2)$ at constant X_{Fe}^{opx} and to high temperature and somewhat elevated pressure with decreasing X_{Fe}^{opx} at constant $X(CO_2)$. Each of the three types of high-grade metamorphosed iron-formation is discussed below. Topologic displacements due to possible uncertainties in the present calculations will be discussed later.

Ol-bearing and Opx-free phase relations (type A)

The phase relations in figure 9 are equivalent to those of type A. Metamorphic temperatures of high-grade iron-formations (type A) have been reported as 600° to 650°C at 2 to 3 kb (Morey and others, 1972; Haase, 1982a). Assemblages of this type (Morey and others, 1972; Bonnichsen, 1975; Floran and Papike, 1978; Haase, 1982a) are siderite-free and are restricted between two curves (7) for $X_{Fe}^{ol} = 0.9$ and for $X_{Fe}^{ol} = 1.0$ (fig. 9A and B). Siderite-free assemblages such as Ol–Gru–Qtz at $X(CO_2) = 0.6$ to 0.9 (1-3 kb, 500°-700°C) are common. A siderite-bearing assemblage such as Ol–Gru–Qtz–Sd (see inset in fig. 10) is limited within temperatures of 430° to 550°C and at $X(CO_2) > 0.9$ (1-3 kb). This temperature limit is the minimum for type A in the presence of quartz, because olivine does not occur below this limit. If $X(CO_2)$ is not sufficiently high (that is, < 0.9) the minimum temperature shifts to 500° to 600°C at 1 to 3 kb, with siderite absent (fig. 13C). The mineral assemblages at pressures above 6 kb may be equivalent to those of type A; these would not be expected in iron-formations but might be encountered in even more Fe-rich bulk compositions.

Opx- and Ol-bearing phase relations (type B)

Type B assemblages in iron-formations are not completely represented in T-$X(CO_2)$ space, because orthopyroxene is unstable below 550°C, and siderite is not stable above 600°C. The T-$X(CO_2)$ conditions may be defined by curve (8) and/or curve (9) at a given X_{Fe}^{opx}. Opx-bearing and siderite-free assemblages such as Opx–Gru–Qtz and Ol–Opx–Gru (Gundersen and Schwartz, 1962; Bonnichsen, 1969, 1975; Simmons, Lindsley, and Papike, 1974; Vaniman, Papike, and Labotka, 1980; and Gole and Klein, 1981) can be located on these curves. The complete phase relations of this type may be demonstrated in more iron-rich rocks where $X_{Fe}^{opx} = 0.9$ at 10 kb. In this case, siderite is stable up to about 720°C. T-P sections for this type are given at $X(CO_2)$ of 0.3 to 0.9 and at fixed $X_{Fe}^{opx} = 0.6$, 0.7, and 0.8 in figure 13, A, B, and C, respectively. In figure 13, A and B, the intersection of curves (7) and (8) (on curve (10)) lies far below 0.5 kb and is therefore not shown. Curve (9) in figure 10 is meta-

stable for iron-formation bulk compositions above the upper pressure limit curve of olivine (dashed lines in fig. 13). It is probable that the assemblage on curve (9) is stable in more Fe-rich rock in which quartz is deficient. The assemblage Ol–Opx–Qtz–Gru (Gole and Klein, 1981) is located near the upper pressure limit. Using these figures, the T-X(CO_2) conditions for type B assemblages can be estimated (fig. 15).

Opx-bearing and Ol-free phase relations (type C)

The assemblages of type C are shown at 6 kb (fig. 12A) and at 10 kb (fig. 12B). The phase relations in these figures are those reported from iron-formation by Butler (1969), Immega and Klein (1976), Dahl (1979), and Klein (1978). Olivine is absent. Siderite-bearing assemblages (Butler, 1969) are generally stable at lower temperatures than siderite-free ones for a fixed pressure (Immega and Klein, 1976; Dahl, 1979). The assemblage Opx–Gru–Qtz–Sd (Butler, 1969) is shown at points P and P′ (fig. 12A). This same area also contains a siderite-free assemblage (Opx–Gru–Qtz) which is located along curve (8). Similar assemblages are also found in the highest grade metamorphosed iron-formations from parts of the southern Labrador Trough (Klein, 1978). The metamorphic conditions are 700° to 750°C and 10 to 11kb. The assemblages of Opx–Gru–Sd–Qtz and Opx–Gru–Qtz are shown at lower X(CO_2) in figure 12B than those in figure 12A. In the same rock unit, the X(CO_2) for the siderite-free assemblage is lower than that for the siderite-bearing one (fig. 12A and B). T-P sections in the T-X(CO_2) space of figure 12, A and B, are shown in figure 13A, B, and C. The phase relations for type C assemblages are located above the upper pressure limit of olivine. Curve (13) for Sd–Qtz–Opx-(X_{Fe}^{opx} = 0.6-0.8) and curve (8) for Gru–Opx–Qtz intersect at the P-T conditions of Butler (1969) where siderite occurs. Figures 12B and 13, however, show that the assemblage at this intersection point does not occur within the P-T conditions of Klein (1978). This implies that, if the temperature is accepted, the grunerite coexisting with siderite and orthopyroxene may be retrograde. The highest X(CO_2) may be estimated in terms of the assemblage on curve 13, at a given P and T.

Using figures 9, 12, and 13, the X(CO_2) of the fluid during regional high-grade metamorphism can be estimated at a given temperature (± 25°C), pressure, and X_{Fe} of the iron-bearing minerals at $P_s = P_{total\ fluid}$, as shown in figure 15. Although the chemical compositions of associated minerals are not available for the rocks of Dahl (1979), the X(CO_2) for his rocks may be estimated to be within the normal range of X_{Fe}^{opx} (0.6 to 0.8).

Topologic displacements due to uncertainties

The thermodynamic properties such as volume, entropy, enthalpy, Gibbs free energy, and heat capacity for all materials used in this study (except grunerite) have a high reliability and are based on X-ray data, calorimetric methods, and other experiments (Robie and others, 1967; Robie, Hemingway, and Fisher, 1978; Robie, Finch, and Hemingway, 1982; Robie, Haselton, and Hemingway, 1984; Helgeson and others,

1978; Miyano and Klein, 1983). PVT data for H_2O and CO_2 from Burnham, Holloway, and Davis (1969) and Shmulovich and Shmonov (1975), respectively, were used. The thermodynamic properties for the gases were derived from these data (Burnham, Holloway, and Davis, 1969; Helgeson and Kirkham, 1974; Fisher and Zen, 1971; Holland, 1981). Errors in the free energies are 0.1 percent or less for H_2O (Helgeson and Kirkham, 1974) and about 0.3 percent for CO_2. Kerrick and Jacobs (1981) calculated the free energies of pure H_2O and CO_2 on the basis of an MRK equation for non-ideal mixing of H_2O and CO_2. They estimated maximum errors of 170 joul for H_2O and 270 joul for CO_2 comparing the free energies calculated from Burnham, Holloway, and Davis (1969) and Shmulovich and Shmonov (1975), respectively. As such, errors for the pure gases are much smaller than those for solid phases. Errors in properties for a gas mixture resulting from the non-ideal mixing model are not well known because of lack of sufficient experimental data. Flowers (1979) showed that the non-ideal mixing model better fits the experiments than the ideal mixing one. Consequently, existing thermodynamic properties and models for fluids generally give reliable results which are consistent with experimental values (also see discussion in Anderson, 1977; and Zen, 1977).

Uncertainties caused by solid solution models as used in this study are difficult to assess because the estimated values from the models for reactions (for example, in fig. 2) cannot be checked by reliable experimental data. We are forced to assume that they are negligible, and as such they are not evaluated in the present calculations.

If we assume that the thermodynamic properties of all materials except grunerite are well known and their errors are negligible, then any final errors are a function of uncertainties derived from grunerite only. Anderson (1977) showed that the maximum error in the free energy change of a reaction derived from an equilibrium P-T bracket is expressed in terms of the product of ΔT and ΔS_r, where ΔT is the temperature difference between lower and upper T at each bracket and ΔS_r is the entropy change of the reaction at equilibrium T and P. Applying this to the P-T brackets of Mel'nik and Radchuk (1977), because of the error in the entropy value of grunerite, the maximum error ϵ_g^{max} in the free energy of reaction (7) at equilibrium P and T can be estimated in terms of the following equation,

$$(\epsilon_g^{max})^2 = \Delta T^2 \{\Delta S_r^2 + (2 \cdot \delta_s)^2\} \quad (5)$$

where δ_s is the uncertainty in the entropy at 25°C of grunerite; no uncertainty in the heat capacity is involved because of its negligible contribution. The larger effect of any errors in the heat capacity is considered below. The calculated value of ϵ_g^{max} is relatively small, namely 4.30 (± 2.15) Kjoul at 0.5 kb (580°C) and 3.19 (± 1.59) Kjoul at 3 kb (650°C), which decreases with increasing pressure because the entropy change becomes smaller. We assume that the error calculated from eq (5) corresponds to the maximum uncertainty δ_g^{max} ($= \pm 1/4\epsilon_g^{max}$) in the free energy of one mole of grunerite at 25°C. If the uncertainty in the heat capacity

of grunerite is considered, the total error ϵ_g^{total} at equilibrium T and P for a reaction involving grunerite can be evaluated by combining with the heat capacity term of Ulbrich and Merino (1974) as follows:

$$(\epsilon_g^{total})^2 = (n \cdot \delta_g^{max})^2 + \left(n \int \delta_{cp}\, dT - n \cdot T \int \frac{\delta_{cp}}{T}\, dT \right)^2 \quad (6)$$

where δ_{cp} denotes uncertainty in the heat capacity of one mole of grunerite in the reaction, n is the mole number of grunerite, and the volume effect of the solids is assumed to be negligible. In order to estimate the maximum discrepancy in the calculated equilibrium temperatures for other reactions, we chose ± 1.08 Kjoul mol^{-1} for the uncertainty in the free energy at 25°C and ± 0.5 percent for that in the heat capacity (average deviation of 0.4 percent in Bennington, Ferrante, and Stuve, 1978) per one mole of grunerite. Using eq (6) and the method of Anderson (1977), because of the heat capacity term, the discrepancy of temperature becomes larger than ± 10°C in the experiment, for instance, ± 17°C at 0.5 kb, ± 27°C at 3 kb, and ± 38°C at 8 kb for curve (7) at Ps = $P(H_2O)$. In the case of reactions in the H_2O-CO_2 gas mixture, the entropy change of a reaction at given P, T, and $X(CO_2)$ is calculated as follows,

$$\Delta S_r\,(T,P,X_{CO_2}) =$$
$$= \Delta S^\circ_r(T) - n_{H_2O} \left\{ \frac{\partial RT \ln(P \cdot X_{H_2O} \cdot \gamma_{H_2O})}{\partial T} \right\}_{P,X_{CO_2}}$$
$$- n_{CO_2} \left\{ \frac{\partial RT \ln(P \cdot X_{CO_2} \cdot \gamma_{CO_2})}{\partial T} \right\}_{P,X_{CO_2}} \quad (7)$$

where $\Delta S^\circ_r(T)$ is the standard entropy change of the reaction, and γ_{H_2O} and γ_{CO_2} are the fugacity coefficients of H_2O and CO_2, respectively, which are calculated from the MRK equation. On the basis of eqs (6) and (7), temperature discrepancies for equilibrium curves at $X_{Fe}^{opx} = 0.8$ (fig. 13C) are computed and summarized in figure 14. Within the range of $X(CO_2) = 0.3$ to 0.9 and at the same temperature and pressure, the temperature discrepancies of the curves at $X_{Fe}^{opx} = 0.6$ (fig. 13A) and 0.7 (fig. 13B) differ by less than 3°C from those in figure 13C, provided that errors derived from the mixing models for solids and fluid are negligible. As we added the difference to the discrepancy for each curve in figure 14 as well, the figure covers the maximum possible displacement of the phase relations independently of the magnitudes of $X(CO_2)$ and X_{Fe}^{opx}. Accordingly, the temperature discrepancies for relevant curves in figures 9 and 12 as well as figure 13, A and B, can be read from figure 14 at a given temperature and pressure. Generally the temperature discrepancy increases most with increasing equilibrium temperature and less with increasing pressure. For curves (7) and (8), the discrepancy at constant X_{Fe}^{opx} decreases with increasing $X(CO_2)$, because their equilibrium temperatures are lowered. The maximum discrepancy of these curves is ± 40°C at $X(CO_2) = 0.3$ and ± 25°C at $X(CO_2) = 0.9$ in P-T space. These values are equivalent

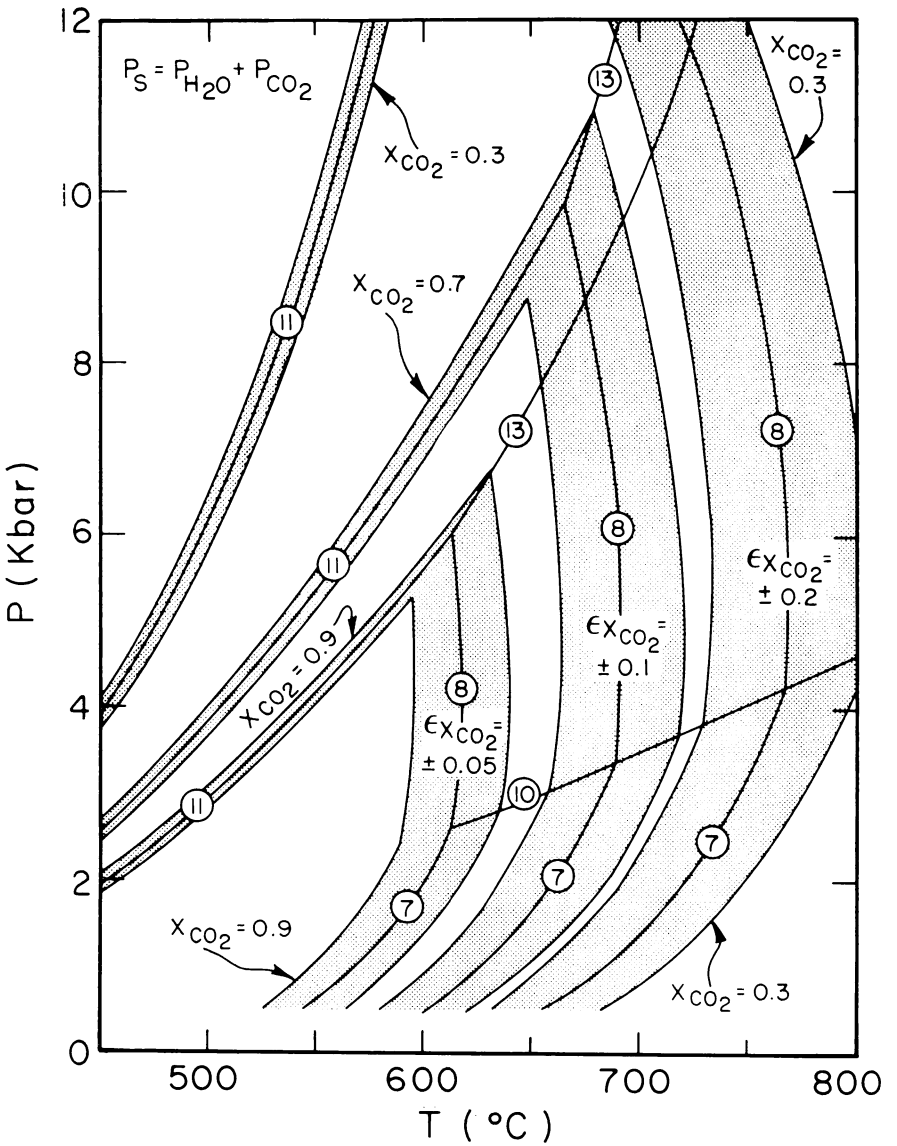

Fig. 14. Possible topologic displacements calculated from uncertainties in the thermodynamic properties of grunerite, using eqs (6) and (7). Although the diagram was constructed at $X_{Fe}^{opx} = 0.8$, with $X(CO_2)$ values ranging from 0.3 to 0.9, it can be applied to estimates of temperature discrepancies in figures 9, 12, 13A and B without dependence on the magnitudes of $X(CO_2)$ and X_{Fe}^{opx}. $\epsilon_{X_{CO_2}}$ denotes equivalent discrepancy in $X(CO_2)$ in T-$X(CO_2)$ space.

to errors in $X(CO_2)$ ($= \epsilon_{XCO_2}$) of about ± 0.2 and ± 0.05, respectively, in T-$X(CO_2)$ space. However, the discrepancy for curve (11) is reduced to less than 5°C because of the large value of entropy of the reaction.

In figure 15, the $X(CO_2)$ of the metamorphic fluid was estimated within ± 25°C of the reported temperature. Thus the estimated error in

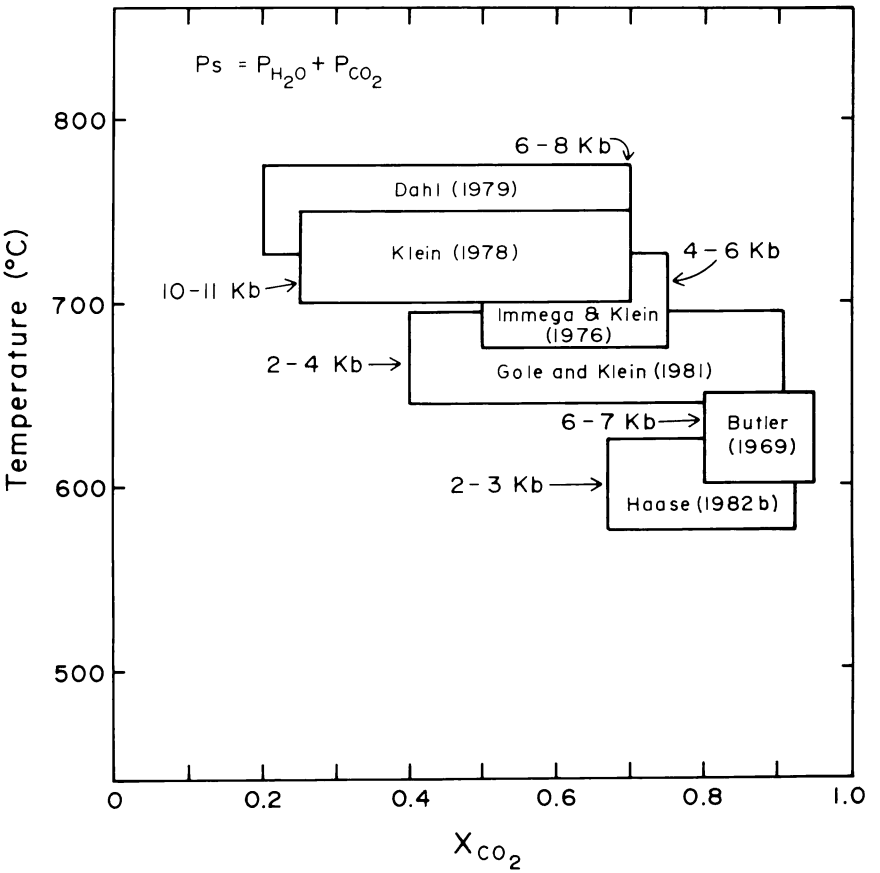

Fig. 15. Fluid compositions ($X(CO_2)$) for various iron-formations. The magnitude of $X(CO_2)$ appears to be a function of mineral compositions (X_{Fe}) rather than temperature and pressure (see text). Data sources are:

Dahl (1979): Opx–Gru–Qtz ($X_{Fe}^{opx} = 0.6$-0.8)

Klein (1978): Opx–Gru–Qtz ± Sd
($X_{Fe}^{opx} = 0.67$-0.83; $X_{Fe}^{Gru} = 0.62$-0.71; $X_{Fe}^{Sd} = 0.72$-0.78).

$X(CO_2$ was estimated from assemblages Gru–Opx–Qtz. The highest $X(CO_2)$ estimated from assemblage Opx–Qtz–Sid ranges up to about 0.93 at 700° and 10 kb.

Immega and Klein (1976): Opx–Gru–Qtz ($X_{Fe}^{opx} = 0.52$-0.71; $X_{Fe}^{Gru} = 0.44$-0.74)

Gole and Klein (1981): Ol–Gru–Qtz ± Opx
($X_{Fe}^{opx} = 0.74$-0.81; $X_{Fe}^{ol} = 0.89$-0.94; $X_{Fe}^{Gru} = 0.72$-0.86)

Butler (1969): Opx–Gru–Qtz ± Sd
($X_{Fe}^{opx} = 0.58$-0.73; $X_{Fe}^{Gru} = 0.53$-0.69; $X_{Fe}^{Sd} = 0.63$)

Haase (1982a): Ol–Gru–Qtz ($X_{Fe}^{ol} = 0.90$-0.96; $X_{Fe}^{Gru} = 0.68$-0.80).

$X(CO_2)$ ranges from ± 0.2 at 750°C to 0.05 at 600°C. However, because of the large uncertainties of more than 50°C in the published metamorphic temperatures (fig. 13), the error in $X(CO_2)$ increases to ± 0.1 to 0.3. However, our conclusions stated below will not be much affected in light of these large temperature uncertainties.

SUMMARY AND CONCLUSIONS

Because the predominant gas species during high-grade metamorphism of iron-formations are H_2O and CO_2, the phase relations in the system Fe–Mg–Si–C–O–H can be treated as a function of X_{Fe} of the Fe-Mg minerals in the binary, mixed-volatile region as well as in T-P space.

The $X(CO_2)$ values for several metamorphic iron-formations are summarized in figure 15. This figure shows that the estimated $X(CO_2)$ for a specific iron-formation varies widely. Generally siderite-bearing assemblages are stable at higher $X(CO_2)$ than siderite-free ones, and assemblages of minerals with high Mg contents are stable at higher $X(CO_2)$ than those with low Mg contents, at a given T and P. In the case of carbonate (siderite)–free iron-formations, the estimated fluid composition may be very CO_2-rich at $Ps = P(CO_2) + P(H_2O)$. Wide variations in the fluid composition in the same rock unit imply steep gradients of H_2O and CO_2 as well as O_2. This would reflect internal control (as immobile components) as noted by many authors (Eugster, 1959; Zen, 1963; Butler, 1969; Klein, 1973, 1978; Frost, 1982; Rice and Ferry, 1982). In a comparison of the various iron-formations in figure 15, the $X(CO_2)$ values may well be a function of the compositions (X_{Fe}) of the iron-bearing minerals rather than of temperature and pressure. However, neither $X(CO_2)$ nor X_{Fe} seem to be the sole and effective control for the formation of siderite in iron-formations. Siderite is stable over limited P-T conditions where an apparent geothermal gradient is smaller than 100°C/kb. However, olivine occurs in metamorphic terrains with a gradient above 150°C/bar. Therefore, in a complete evaluation of paragenetic variations of high-grade metamorphic minerals one must also assess the effect of the magnitude of a possible geothermal gradient during metamorphism.

ACKNOWLEDGMENTS

This research was made possible by a Grant-in-Aid of the University of Tsukuba (to T.M.). Further finding was supported by NSF grants EAR-80-20377, EAR-82-05473, EAR8419161, and EAR8415681 (to C.K.). Special thanks are due to Y. Suzuki and T. Fujii at the University of Tsukuba for their helpful suggestions and encouragements. We are grateful to Donald M. Burt, Eric J. Essene, B. Ronald Frost, C. S. Haase, and A. B. Thompson for constructive comments on various versions of this manuscript. The illustrations were drafted by Joel P. Grimm and Elaine Stewart at the University of New Mexico.

References

Anderson, G. M., 1977, The accuracy and precision of calculated mineral dehydration equilibria, *in* Fraser, D. G., ed., Thermodynamics in Geology: Boston, Mass., D. Reidel, p. 115-136.

Anovitz, L. C., and Essene, E. J., 1986, Phase equilibria in the system $CaCO_3$–$MgCO_3$–$FeCO_3$: Jour. Petrology, in press.

Bennington, K. O., Ferrante, M. J., and Stuve, J. M., 1978, Thermodynamic data on the amphibole asbestos minerals amosite and crocidolite: U.S. Bur. Mines Rept. Inv. 8265, 29 p.

Bohlen, S. R., and Boettcher, A. L., 1981, Experimental investigations and geological applications of orthopyroxene geothermometry: Am. Mineralogist, v. 66, p. 951-964.

Bonnichsen, B., 1969, Metamorphic pyroxenes and amphiboles in the Biwabik Iron Formation, Dunka River area, Minnesota: Mineralog. Soc. America Spec. Paper 2, p. 217-239.

———— 1975, Geology of the Biwabik Iron Formation, Dunka River area, Minnesota: Econ. Geology, v. 70, p. 319-340.

Burnham, C. W., Holloway, J. R., and Davis, N. F., 1969, Thermodynamic properties of water to 1000°C and 10,000 bars: Geol. Soc. America Spec. Paper 132, 96 p.

Burt, D. M., 1972, The system Fe–Si–C–O–H: A model for metamorphosed iron-formations: Carnegie Inst. Washington Year Book 71, p. 435-443.

Butler, P. M., 1969, Mineral compositions and equilibria in the metamorphosed iron-formation of the Gagnon region, Quebec, Canada: Jour. Petrology, v. 10, p. 56-101.

Chakraborty, K. L., 1966, Ferromagnesian silicate minerals in the metamorphosed iron-formations of Wabush Lake and adjacent areas, Newfoundland and Quebec: Canada Geol. Survey Bull. 143, 34 p.

Chatillon-Colinet, C., Newton, R. C., Perkins III, D., and Kleppa, J., 1983, Thermochemistry of $(Fe^{2+},Mg)SiO_3$ orthopyroxene: Geochim. et Cosmochim. Acta, v. 47, p. 1957-1603.

Dahl, P. S., 1979, Comparative geothermometry based on major-element and oxygen isotope distributions in Precambrian metamorphic rocks from southwestern Montana: Am. Mineralogist, v. 64, p. 1280-1293.

Engi, M., 1980, The solid solution behavior of olivine in the temperature-range from 500K to 1500K [abs.]: Geol. Soc. America, Abs. with Programs, v. 12, 421.

Eugster, H. P., 1959, Oxidation and reduction in metamorphism, *in* Abelson, P. H., ed., Researches in Geochemistry, v. 1: New York, John Wiley & Sons, p. 397-426.

———— 1977, Compositions and thermodynamics of metamorphic solutions, *in* Fraser, D. G., ed., Thermodynamics in Geology: Boston, Mass., D. Reidel, p. 183-202.

Eugster, H. P., and Skippen, G. B., 1967, Igneous and metamorphic reactions involving gas equilibria, *in* Abelson, P. H., ed., Researches in Geochemistry, v. 2: New York, John Wiley & Sons, p. 492-520.

Ferry, J. M., and Burt, D. M., 1982, Characterization of metamorphic fluid composition through mineral equilibria, *in* Ferry, J. M., ed., Characterization of Metamorphism through Mineral Equilibria: Mineralog. Soc. America, Rev. in Mineralogy, v. 10, p. 207-262.

Fisher, J. R., and Zen, E., 1971, Thermodynamic calculations from hydrothermal phase equilibrium data and the free energy of H_2O: Am. Jour. Sci., v. 270, p. 297-314.

Floran, R. J., and Papike, J. J., 1978, Mineralogy and petrology of the Gunflint Iron Formation, Minnesota-Ontario: Correlation of compositional and assemblage variations at low to moderate grade: Jour. Petrology, v. 19, p. 215-288.

Flowers, G. C., 1979, Correction of Holloway's (1977) adaption of the modified Redlich-Kwong equation of state for calculation of the fugacities of molecular species in supercritical fluids of geologic interest: Contr. Mineralogy Petrology, v. 48, p. 89-114.

Fonarev, V. I., 1981a, Thermodynamic functions of olivine and orthopyroxene solid solutions: Geochem. Internat., v. 18(4), p. 142-157.

———— 1981b, Thermodynamic functions of cummingtonite solid solutions: Geochem. Internat., v. 18(5), p. 1-11.

Fonarev, V. I., and Korolkov, G. Ya., 1980, The assemblage orthopyroxene + cummingtonite + quartz. The low-temperature stability limit: Contr. Mineralogy Petrology, v. 73, p. 413-420.

Fonarev, V. I., Korolkov, G. Ya., and Dokina, T. N., 1976, Stability of the cummingtonite–quartz–magnetite association: Geochem. Internat., v. 13, p. 34-35.

———— 1979, Cummingtonite + olivine + quartz association: Geochem. Internat., v. 16, p. 21-32.

Forbers, W. C., 1977, Stability relations of grunerite, $Fe_7Si_8O_{22}(OH)_2$: Am. Jour. Sci., v. 277, p. 735-749.

French, B. M., 1966, Some geological implications of equilibrium between graphite and a C–H–O gas phase at high temperatures and pressures: Rev. Geophysics, v. 4, p. 223-253.

———— 1968, Progressive contact metamorphism at the Biwabik Iron Formation, Mesabi Range, Minnesota: Minnesota Geol. Survey Bull., v. 45, 103 p.

———— 1971, Stability relations of siderite ($FeCO_3$) in the system Fe–C–O: Am. Jour. Sci., v. 271, p. 37-78.

Frost, B. R., 1979a, Metamorphism of iron-formation: paragenesis in the system Fe–Si–C–O–H: Econ. Geology, v. 74, p. 775-785.

———— 1979b, Mineral equilibria involving mixed volatiles in a C–O–H fluid: the stabilities of graphite and siderite: Am. Jour. Sci., v. 279, p. 1033-1059.

———— 1982, Contact metamorphic effects of the Stillwater Complex: the concordant iron-formation: a discussion of the role of buffering in metamorphism of iron-formation: Am. Mineralogist, v. 67, p. 142-149.

Ganguly, J., 1982, Thermodynamics, kinetics, and geological applications of Mg–Fe order-disorder in ferromagnesian silicates, *in* Saxena, S. K., ed., Advances in Physical Geochemistry v. 2: New York, Springer-Verlag, p. 58-99.

Ghose, S., 1981, Subsolidus reactions and microstructures in amphiboles, *in* Veblen, D. R., ed., Amphiboles and other hydrous pyriboles, *in* Reviews in Mineralogy v. 9A: Mineralog. Soc. America, p. 325-372.

Ghose, S., and Weidner, J. R., 1971, Mg^{2+}–Fe^{2+} distribution isotherms in cummingtonites at 600 and 700 C [abs.]: EOS, v. 52, p. 381.

Gole, M. J., and Klein, C., 1981, High-grade metamorphic Archean banded iron-formations, Western Australia: assemblages with coexisting pyroxenes ± fayalite: Am. Mineralogist, v. 66, p. 87-99.

Gundersen, J. N., and Schwartz, G. M., 1962, The geology of the metamorphosed Biwabik Iron-Formation, Eastern Mesabi District, Minnesota: Minnesota Geol. Survey Bull., v. 43, 139 p.

Haase, C. S., 1982a, Metamorphic petrology of the Negaunee Iron Formation, Marquette district, northern Michigan: mineralogy, metamorphic reactions and phase equilibria: Econ. Geology, v. 77, p. 60-81.

———— 1982b, Phase equilibria in metamorphosed iron-formations: qualitative T-X(CO_2) petrologic grids: Am. Jour. Sci., v. 282, p. 1623-1654.

Hafner, S. S., and Ghose, S., 1971, Iron and magnesium distribution in cummingtonites $(Fe,Mg)_7Si_8O_{22}(OH)_2$: Zeitschr. Kristallographie, v. 133, p. 301-326.

Helgeson, H. C., Delany, J. M., Nesbitt, H. W., and Bird, D. K., 1978, Summary and critique of the thermodynamic properties of rock-forming minerals: Am. Jour. Sci., v. 278-A, 229 p.

Helgeson, H. C., and Kirkham, D. H., 1974, Theoretical prediction of the thermodynamic behavior of aqueous electrolytes at high pressures and temperatures. I. Summary of the thermodynamic/electrostatic properties of the solvent: Am. Jour. Sci., v. 274, p. 1089-1198.

Holland, T. J. B., 1981, Thermodynamic analysis of simple mineral systems, *in* Newton, R. C., Navrotsky, A., and Wood, B. J., eds., Thermodynamics of Minerals and Melts: New York, Springer-Verlag, p. 19-34.

Holloway, J. R., 1977, Fugacity and activity of molecular species in supercritical fluids, *in* Fraser, D. G., ed., Thermodynamics in Geology: Boston, Mass., D. Reidel, p. 161-181.

———— 1981, Compositions and volumes of supercritical fluids in the Earth's crust, *in* Hollister, L. S., and Crawford, M. L., eds., Fluid Inclusions: Applications to Petrology: Calgary, Mineralog. Assoc. Canada, p. 13-38.

Immega, I. P., and Klein, C., 1976, Mineralogy and petrology of some metamorphic Precambrian iron-formations in southwestern Montana: Am. Mineralogist, v. 61, p. 1117-1144.

Kawasaki, T., and Matsui, Y., 1977, Partitioning of Fe^{2+} and Mg^{2+} between olivine and garnet: Earth Planetary Sci. Letters, v. 37, p. 159-166.

Kerrick, D. M., 1974, Review of metamorphic mixed-volatile (H_2O–CO_2) equilibria: Am. Mineralogist, v. 59, p. 729-762.

Kerrick, D. M., and Jacobs, G. K., 1981, A modified Redlich-Kwong equation for H_2O, CO_2, and H_2O–CO_2 mixtures at elevated pressures and temperatures: Am. Jour. Sci., v. 281, p. 735-767.

Kitayama, K., and Katsura, T., 1968, Activity measurements in orthosilicate and metasilicate solid solutions — I. Mg_2SiO_4–Fe_2SiO_4 and $MgSiO_3$–$FeSiO_3$ at 1204°C: Chem. Soc. Japan Bull., v. 41, p. 1146-1151.

Klein, C., 1966, Mineralogy and petrology of the metamorphosed Wabush Iron-Formation, southwestern Labrador: Jour. Petrology, v. 7, p. 246-305.

———— 1973, Changes in mineral assemblages with metamorphism of some banded Precambrian iron-formations: Econ. Geology, v. 68, p. 1075-1088.

———— 1978, Regional metamorphism of Proterozoic iron-formations, Labrador and the Province of Quebec, Canada: Am. Mineralogist, v. 63, p. 898-912.

———— 1983, Diagenesis and metamorphism of Precambrian banded iron-formations, *in* Trendall, A. F., and Morris, R. C., eds., Iron-formation: Facts and problems: New York, Elsevier, p. 417-469.

Kranck, S. H., 1961, A study of the phase equilibria in a metamorphic iron-formation: Jour. Petrology, v. 2, p. 137-184.

Matsui, Y., and Nishizawa, O., 1974, Iron(II)-magnesium exchange equilibrium between olivine and calcium-free pyroxene over a temperature range 800°C to 1300°C: Soc. française Mineralogie Cristallographie Bull., v. 97, 122-130.

Matsumoto, T., 1971, Pressure-temperature conditions for the formation of peridotite inclusions. An application of a regular solution model to partitioning of Mg, Fe, and Co between existing olivine and orthopyroxene: Geochem. Jour., v. 4, p. 111-121.

Mel'nik, Yu. P., and Radchuk, V. V., 1977, The stability of grunerite–$Fe_7Si_8O_{22}(OH)_2$: Geokhimiya, v. 5, p. 693-704 (in Russian).

Mel'nik, Yu. P., and Siroshtan, R. I., 1973, Physico-chemical conditions of the metamorphism of cherty-iron rocks, *in* Genesis of Precambrian iron and manganese deposits: Kiev Symposium, 1970 (Earth Sci. 9), Paris, UNESCO, Proc. p. 209-216.

Miyano, T., 1976, Physicochemical environments during burial metamorphism of the Dales Gorge Member, Hamersley Group, Western Australia (in Japanese with English abstract): Mining Geology of Japan, v. 26, p. 311-325.

———— 1978a, Effect of CO_2 on mineralogical differences in some low-grade metamorphic iron-formations: Geochem. Jour., v. 12, p. 201-211.

———— 1978b, Phase relations in the system Fe–Mg–Si–O–H and environments during low-grade metamorphism of some Precambrian iron-formations: Geol. Soc. Japan Jour., v. 84, p. 679-690.

———— 1978c, Stability relations of iron-bearing minerals in the H_2O–CO_2 mixed-volatile region at lower temperatures: Geol. Soc. Japan Jour., v. 84, p. 711-719.

Miyano, T., and Klein, C., 1983, Phase relations of orthopyroxene, olivine, and grunerite in high-grade metamorphic iron-formation: Am. Mineralogist, v. 68, p. 699-716.

Morey, G. B., Papike, J. J., Smith, R. W., and Weiblen, P. W., 1972, Observations on the contact metamorphism of the Biwabik Iron-formation, East Mesabi District, Minnesota: Geol. Soc. America Mem. 135, p. 225-264.

Mueller, R. F., 1962, Energetics of certain silicate solid solutions: Geochim. et Cosmochim. Acta, v. 26, p. 265-275.

———— 1973, System CaO–MgO–FeO–SiO_2–C–H_2–O_2: some correlations from nature and experiment: Am. Jour. Sci., v. 273, p. 152-170.

Nafziger, R. H., and Muan, A., 1967, Equilibrium phase compositions and thermodynamic properties of olivines and orthopyroxenes in the system MgO–"FeO"–SiO_2: Am. Mineralogist, v. 52, p. 1364-1385.

Navrotsky, A., 1971, The intracrystalline cation distribution and the thermodynamics of solid solution formation in the system $FeSiO_3$–$MgSiO_3$: Am. Mineralogist, v. 56, p. 201-211.

———— 1978, Thermodynamics of element partitioning: (1) Systematics of transition metals in crystalline and molten silicates and (2) defect chemistry and "Henry's law problem": Geochim. et Cosmochim. Acta, v. 42, p. 887-902.

Ohmoto, H., and Kerrick, D., 1977, Devolatilization equilibria in graphitic schists: Am. Jour. Sci., v. 277, p. 1013-1044.

O'Neill, H. St. C., and Wood, B. J., 1979, An experimental study of Fe–Mg partitioning between garnet and olivine and its calibration as a geothermometer: Contr. Mineralogy Petrology, v. 70, p. 59-70.

Perchuk, L. L., 1977, Thermodynamic control of metamorphic processes, *in* Saxena, S. K., and Bhattacharji, S., eds., Energetics of Geological Processes: New York, Springer-Verlag, p. 285-352.

Rice, J. M., and Ferry, J. M., 1982, Buffering, infiltration, and the control of intensive variables during metamorphism, *in* Ferry, J. M., ed., Characterization of Metamorphism Through Mineral Equilibria: Mineralog. Soc. America, Rev. in Mineralogy, v. 10, p. 263-326.

Robie, R. A., Bethke, P. M., Toulmin, M. S., and Beardsley, K. M., 1967, Selected X-ray crystallographic data molar volumes, and densities of minerals and related substances: U.S. Geol. Survey Bull. 1248, 87 p.

Robie, R. A., Finch, C. B., and Hemingway, B. S., 1982, Heat capacities and entropy of fayalite (Fe_2SiO_4) between 5.1 and 383 K: comparison of calorimetric and equilibrium values for the QFM buffer reaction: Am. Mineralogist, v. 67, p. 463-469.

Robie, R. A., Haselton, H. T., Jr., and Hemingway, B. S., 1984, Heat capacities and entropies of rhodochrosite ($MnCO_3$) and siderite ($FeCO_3$) between 5 and 600 K: Am. Mineralogist, v. 69, p. 349-357.

Robie, R. A., Hemingway, B. S., and Fisher, J. R., 1978, Thermodynamic properties of minerals and related substances at 298.15 K and 1 bar (10^5 Pascals) pressure and at higher temperatures: U.S. Geol. Survey Bull. 1452, 456 p.

Sack, R. O., 1980, Some constraints on the thermodynamic mixing properties of Fe–Mg orthopyroxenes and olivines: Contr. Mineralogy Petrology, v. 71, p. 257-269.

Saxena, S. K., 1973, Thermodynamics of rock-forming crystalline solutions: New York, Springer-Verlag, 188 p.

———— 1982, Computation of multicomponent phase equilibria: *in* Saxena, S. K., Advances in Physical Geochemistry, v. 2: New York, Springer-Verlag, p. 225-241.

Seguin, M. K., 1971, Phase relations in the Fe–C–O–S–H_2O system and its geological application: Chem. Geology, v. 7, p. 5-18.

Shmulovich, K. I., and Shmonov, V. M., 1975, Fugacity coefficients of CO_2 from 1.0132 to 10,000 bars and from 450 to 1300 K: Geochimica, v. 1, p. 551-555.

Simmons, E. C., Lindsley, D. H., and Papike, J. J., 1974, Phase relations and crystallization sequence in a contact-metamorphosed rock from the Gunflint Iron-Formation, Minnesota: Jour. Petrology, v. 15, p. 539-565.

Ulbrich, H. H., and Merino, E., 1974, An examination of standard enthalpies of formation of selected minerals in the system SiO_2–Al_2O_3–K_2O–Na_2O–H_2O: Am. Jour. Sci., v. 274, p. 519-542.

Vaniman, D. T., Papike, J. J., and Labotka, T., 1980, Contact-metamorphic effects of the Stillwater Complex, Montana: the concordant iron-formation: Am. Mineralogist, v. 65, p. 1087-1102.

Weidner, J. R., 1972, Equilibria in the system Fe–C–O part I: Siderite–magnetite–carbon-vapor equilibrium from 500 to 10,000 bars: Am. Jour. Sci., v. 272, p. 735-751.

Williams, R. J., 1972, Activity-composition relations in the fayalite–forsterite solid solution between 900 and 1300°C at low pressures: Earth Planetary Sci. Letters, v. 15, p. 296-300.

Wood, B. J., and Kleppa, O. J., 1981, Thermochemistry of forsterite–fayalite olivine solutions: Geochim. et Cosmochim. Acta, v. 45, p. 529-534.

Zen, E., 1963, Components, phases, and criteria of chemical equilibrium in rocks: Am. Jour. Sci., v. 261, p. 929-942.

———— 1966, Construction of pressure-temperature diagrams for multi-component systems after the method of Schreinemakers — a geometric approach: U.S. Geol. Survey Bull. 1225, 55 p.

———— 1972, Gibbs free energy, enthalpy, and entropy of ten rock-forming minerals: calculations, discrepancies, implications: Am. Mineralogist, v. 57, p. 534-553.

———— 1977, The phase equilibrium calorimeter, the petrologic grid, and a tyranny of numbers: Am. Mineralogist, v. 62, p. 189-204.